Late Neoproterozoic paleogeography of the Southeastern New England Avalon Zone: Insights from U-Pb geochronology and paleomagnetism

M.D. Thompson†
Department of Geosciences, Wellesley College, Wellesley, Massachusetts 02481, USA

A.M. Grunow‡
Byrd Polar Research Center, Ohio State University, Columbus, Ohio 43210, USA

J. Ramezani§
Department of Earth, Atmospheric and Planetary Sciences, Massachusetts Institute of Technology, Cambridge, Massachusetts 02139, USA

ABSTRACT

Integrated geochronologic and paleomagnetic investigation of the arc-related Lynn and Mattapan volcanic complexes around Boston, Massachusetts, establishes a Neoproterozoic paleopole for the Southeastern New England Avalon Zone. Four new U-Pb zircon dates obtained using isotope dilution and thermal ionization mass spectrometry (ID-TIMS) methods range from 597.4 ± 1.5 Ma to 595.7 ± 1.6 Ma, in agreement with published Lynn-Mattapan results of ca. 596 Ma. The mean direction calculated from the A component of magnetization at nine Lynn-Mattapan sites has a declination (D) of 319.9° and an inclination (I) of 57.0° (α95 = 7.4°); the paleopole based on this mean direction is 206°E, 60°N. These results pass both reversals and fold tests and are regionally consistent among lithologies that include basalt, andesite, rhyodacite, and rhyolite, which represent both volcanic and subvolcanic phases. Most sites also contain stable B and C magnetic components with directions that suggest Ordovician to Permian remagnetizations. A broadly comparable A component direction with D = 109.0° and I = –63.4° (α95 = 9.4°, *n* = 11 samples) was obtained from one site in the Squantum Member of the Roxbury Conglomerate (maximum age of 593 Ma) overlying the volcanic sequence.

The Lynn-Mattapan results indicate that southeastern New England occupied a mid-latitude position at ca. 595 Ma, similar to those reported from Avalonian terranes in maritime Canada. The most likely peri-Gondwanan position for Avalonia consistent with these paleomagnetic data lies off the West African margin. Using poles from the East Sahara craton (Egypt) and the Rio de la Plata craton (Brazil) has permitted reconstruction of West Gondwana without recourse to Laurentian proxies.

Keywords: Avalon Zone, New England, Neoproterozoic, U-Pb geochronology, paleopole, paleogeography.

INTRODUCTION

Paleomagnetic arguments have long placed Avalonian terranes of Newfoundland, Nova Scotia, New Brunswick, and southeastern New England adjacent to northern Gondwana during the Neoproterozoic (Van der Voo, 1982, 1993; Torsvik et al., 1996), but the exact configuration has never been resolved. Geological thinking on this issue originally emphasized similarities between Avalonian magmatic rocks and Pan-African sequences in northern Africa (Rast and Skehan, 1983; Hermes and Zartman, 1992). Later interpretations, however, have increasingly favored an Amazonian position (Nance and Murphy, 1994, 1996; van Staal et al., 1996; Keppie et al., 1998) on the basis of Nd basement isotopic signatures of crystalline rocks and detrital zircon suites containing 1.0–1.3 Ga components that could have been derived from South American source belts. Recent paleomagnetic results from 580 to 570 Ma volcanic and sedimentary rocks of the Marystown Group in the Burin Peninsula, southeastern Newfoundland (McNamara et al., 2001) have reenergized the West African versus Amazonian debate (Murphy et al., 2002; MacNiocaill et al., 2002; Murphy et al., 2004). One common feature of the reconstructions presented by all parties in this discussion is the assumed late Neoproterozoic juxtaposition of Laurentia, Amazonia, and West Africa and the corollary acceptance of Neoproterozoic Laurentian poles as paleomagnetic proxies for the Gondwanan cratonic elements. Difficulties with this approach are compounded by ambiguities over high versus low latitude of Laurentia during the late Neoproterozoic (Pisarevsky et al., 2000). This paper presents integrated paleomagnetic and geochronologic results from ca. 595 Ma arc-related volcanic rocks in the Southeastern New England Avalon Zone around Boston, Massachusetts (Fig. 1), that provide a new, precisely dated paleomagnetic pole bearing on this problem. This pole and Canadian poles discussed in comparison all derive from terranes belonging to Avalonia as delineated on the *Lithotectonic Map of the Appalachian Orogen* (Hibbard et al., 2006). Peri-Gondwanan terranes assigned to Ganderia because of their slightly different Neoproterozoic histories (recent review in Hibbard, 2004) are not considered in our analysis.

REGIONAL GEOLOGY AND PREVIOUS AGE CONSTRAINTS

Magmatic rocks in the Southeastern New England Avalon Zone record plutonism and volcanism between ca. 625 Ma and 590 Ma (regional U-Pb zircon geochronology reviewed in Thompson et al., 1996). Intrusive activity in the greater Boston area (Fig. 1) is represented by the widespread ca. 610 Ma Dedham Granite (Hepburn et al., 1993; Ault et al., 2004) and the localized, ca. 599 Ma Westwood Granite (Thompson et al., 1996). Surface eruptions are recorded in dominantly siliceous volcanic rocks, locally associated with andesite and basalt, called the Lynn Volcanic Complex north of Boston and the Mattapan Volcanic Complex

†E-mail address: mthompson@wellesley.edu.
‡E-mail address: grunow.1@osu.edu.
§E-mail address: ramezani@mit.edu.

GSA Bulletin; May/June 2007; v. 119; no. 5/6; p. 681–696; doi: 10.1130/B26014.1; 7 figures; 5 tables; Data Repository item 2007065.

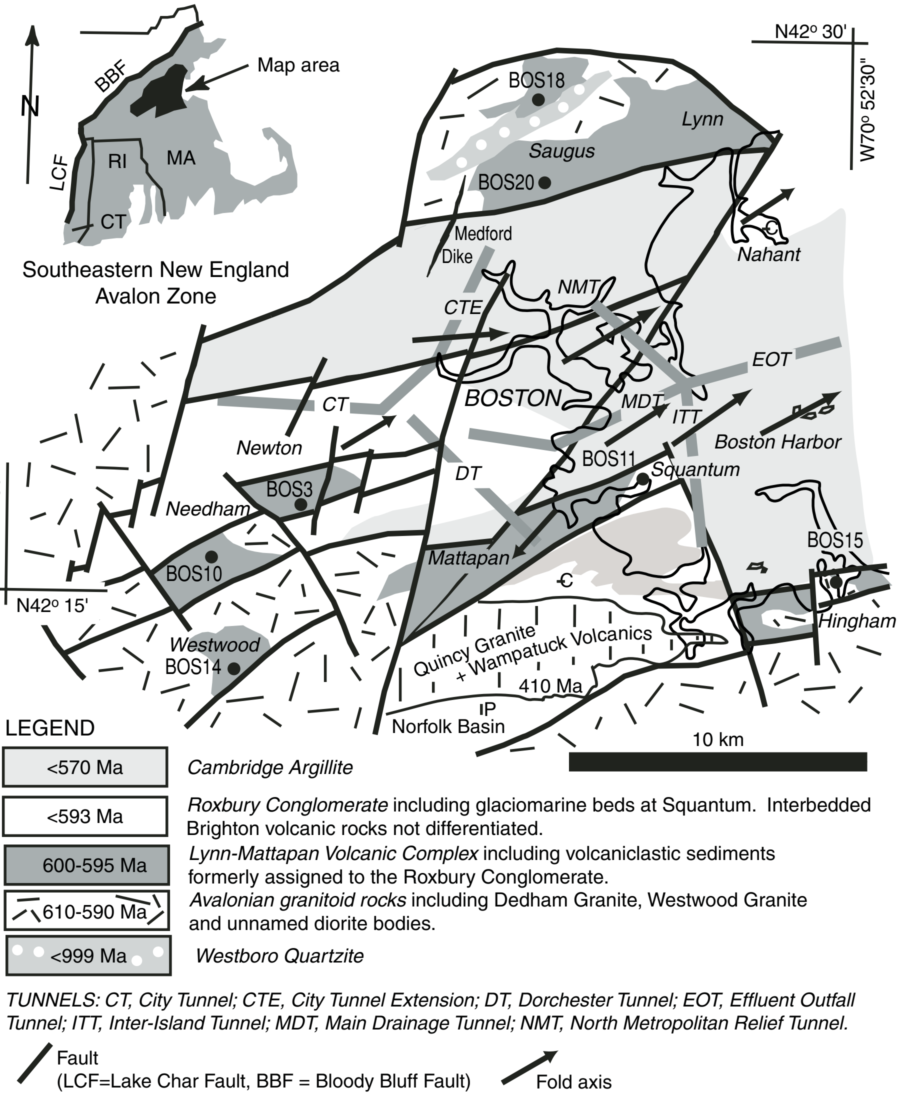

Figure 1. Schematic geologic map of the Southeastern New England Avalon Zone around Boston, Massachusetts, adapted from Billings (1976), Zen (1983), Thompson (1993), and unpublished field and subsurface data. Legend shows only Neoproterozoic units; younger units are labeled in map itself. U-Pb ages from Kaye and Zartman (1980), Hepburn et al. (1993), Thompson et al. (1996), Thompson and Bowring (2000), and this paper. Sampling sites are indicated by solid circles.

to the south (LaForge, 1932; Zen, 1983). Subsequent work recognizes great diversity among these units, including ash-flow tuffs, caldera-collapse breccias (Thompson, 1985; Thompson and Hermes, 1990), subvolcanic intrusive phases (Smith and Hon, 1984), and associated volcaniclastic sediments (Ault, 2003). However, recently published U-Pb dates indicate similar ages across the region: Mattapan rhyodacite from Westwood, Massachusetts (BOS14 in Figure 1; analysis 1 in Table DR1[1]), yields an upper concordia intercept date of 596 ± 2 Ma (Thompson et al., 1996), and Lynn rhyolite from a quarry operated by Aggregate Industries in Saugus, Massachusetts (BOS20 in Figure 1; analysis 2 in Table DR1), is constrained at ca. 596 Ma by a concordant zircon fraction (Hepburn et al., 1993).

The plutonic and volcanic rocks just described are overlain in the Boston Basin by the Roxbury Conglomerate, which is traditionally divided, in ascending order, into the Brookline, Dorchester, and Squantum Members (Emerson, 1917; LaForge, 1932; Billings, 1976). The Squantum sequence (BOS11 in Fig. 1) is largely reddish to purplish siltstone, sandstone, and conglomerate, but also includes boulder-bearing diamictite originally interpreted as glacial till (Sayles and LaForge, 1910; Sayles, 1914). The "tillite" is now generally viewed as debris flow deposits, as first argued by Pettijohn (1957) and Dott (1961), but glacial influence during Squantum deposition remains probable on the basis of lonestones interpreted as ice-rafted debris in associated siltstones (Socci and Smith, 1990; Smith and Socci, 1990). The northeast-striking, moderately south-dipping Squantum section is folded about a shallowly SSW-plunging fold axis and exhibits a well-developed spaced cleavage.

The Squantum beds are the only portion of the Roxbury Conglomerate currently constrained by U-Pb geochronology (Thompson and Bowring, 2000). Nine single zircons from a poorly sorted, lithic-rich sandstone at the base of the 190 m stratigraphic section yield generally concordant $^{207}Pb/^{206}Pb$ dates ranging from ca. 618 Ma to ca. 593 Ma, and three igneous clasts from diamictite higher in the section have been dated at ca. 610 Ma, ca. 600 Ma, and ca. 596 Ma. Based on these results, Squantum deposition is younger than ca. 593 Ma.

The youngest Neoproterozoic strata in the Boston Basin comprise thousands of meters of monotonously laminated gray mudstone and siltstone assigned to the Cambridge Argillite (Emerson, 1917; LaForge, 1932; Billings, 1976). In the northern half of the Boston Basin, this sequence contains *Bavlinella* cf. *faveolata* (Lenk et al., 1982), microfossils described as most common (Vidal, 1976) in deposits of Vendian age (Ediacaran Period of Knoll et al., 2004). A volcanic ash bed estimated (owing to intervening faults) to lie ~500 m below the fossil locality has yielded a range of zircon dates the youngest of which is a concordant analysis at 570 Ma (Thompson and Bowring, 2000). In conjunction with the microfossils, this seems to be a good estimate of the age of the ash bed, but it is impossible to rule out the presence of even younger zircons, given the dominance of inherited or xenocrystic grains with $^{207}Pb/^{206}Pb$ dates that range back to 696 Ma. The Cambridge Argillite and Roxbury Conglomerate are jointly known as the Boston Bay Group (Emerson, 1917; LaForge, 1932; Billings, 1976; Zen, 1983).

Late Paleozoic Alleghanian tectonism can be detected in the Cambridge Argillite as well as in overlying Cambrian platform deposits (Fig. 1) along the southern margin of the Boston Basin. These units are deformed by WSW-plunging folds with steep to overturned limbs like those that affect fossiliferous Pennsylvanian rocks in the adjoining Norfolk Basin (south edge of

[1]GSA Data Repository item 2007065, major and trace element geochemistry, is available on the Web at http://www.geosociety.org/pubs/ft2007.htm. Requests may also be sent to editing@geosociety.org.

TABLE 1. U-Pb ISOTOPIC DATA FOR LYNN-MATTAPAN VOLCANIC ROCKS IN THE VICINITY OF BOSTON, MASSACHUSETTS

						Ratios						Age (Ma)			
Sample Fractions†	Pb_c‡ (pg)	Pb^*/Pb_c‡	Th/U	$^{206}Pb/^{204}Pb$§	$^{208}Pb/^{206}Pb$#	$^{206}Pb/^{238}U$††	Error (2σ%)	$^{207}Pb/^{235}U$††	error (2σ%)	$^{207}Pb/^{206}Pb$††	Error (2σ%)	$^{206}Pb/^{238}U$	$^{207}Pb/^{235}U$	$^{207}Pb/^{206}Pb$	Corr. coef.
Rhyolite porphyry, Saugus (MT95-1)															
z1	0.5	94.0	0.41	5530.4	0.150	0.228616	(.08)	3.14683	(.10)	0.09983	(.06)	1327.2	1444.2	1620.9	0.793
z2	0.3	89.4	0.47	5445.6	0.147	0.098625	(.08)	0.81705	(.10)	0.06008	(.06)	606.3	606.4	606.6	0.802
z3	0.6	10.2	1.34	522.3	0.418	0.096771	(.37)	0.79864	(.59)	0.05986	(.44)	595.5	596.1	598.4	0.677
z4	0.7	47.5	0.82	2661.9	0.256	0.096841	(.11)	0.79863	(.18)	0.05981	(.14)	595.9	596.1	596.8	0.650
z5	0.4	30.9	1.15	1611.7	0.358	0.096877	(.13)	0.79863	(.22)	0.05979	(.17)	596.1	596.1	596.0	0.636
z6	0.3	22.1	1.01	1194.5	0.315	0.096730	(.18)	0.79738	(.28)	0.05979	(.20)	595.2	595.4	595.9	0.683
z7	0.3	28.5	1.10	1510.3	0.337	0.096811	(.15)	0.79524	(.27)	0.05958	(.21)	595.7	594.1	588.2	0.618
z8	0.5	33.4	1.05	1780.5	0.327	0.096215	(.14)	0.79250	(.23)	0.05974	(.18)	592.2	592.6	594.1	0.649
z9	0.6	18.5	1.07	989.3	0.333	0.096036	(.21)	0.79079	(.32)	0.05972	(.23)	591.1	591.6	593.5	0.697
Rhyolite porphyry, Newton (MT01-28)															
z10	2.1	50.1	0.89	2808.5	0.280	0.095640	(.27)	0.78919	(.35)	0.05985	(.22)	588.8	590.7	598.1	0.781
z11	0.8	80.7	0.88	4530.2	0.277	0.096389	(.09)	0.79521	(.11)	0.05983	(.07)	593.2	594.1	597.6	0.762
z12	1.3	80.7	0.87	4542.6	0.274	0.096260	(.14)	0.79386	(.15)	0.05981	(.07)	592.5	593.4	596.8	0.899
z13	1.3	27.4	0.79	1578.7	0.252	0.096708	(.17)	0.80166	(.29)	0.06012	(.23)	595.1	597.8	607.9	0.606
z14	1.0	48.5	0.87	2736.0	0.273	0.096336	(.09)	0.79499	(.13)	0.05985	(.09)	592.9	594.0	598.2	0.727
z15	1.1	23.7	0.83	1357.9	0.261	0.096462	(.19)	0.79550	(.32)	0.05981	(.25)	593.6	594.3	596.8	0.621
Rhyolitic ash-flow tuff, Needham (MT-KK10)															
z16	4.1	24.8	0.99	1343.2	0.312	0.096146	(.34)	0.79346	(.38)	0.05985	(.16)	591.8	593.1	598.3	0.911
z17	15.1	19.6	0.80	1135.5	0.252	0.096089	(.19)	0.79293	(.29)	0.05985	(.21)	591.4	592.8	598.1	0.699
z18	2.8	21.9	1.05	1194.0	0.334	0.096155	(.21)	0.79583	(.52)	0.06003	(.46)	591.8	594.5	604.6	0.473
z19	0.8	97.2	0.90	5439.2	0.280	0.096624	(.06)	0.79639	(.09)	0.05978	(.07)	594.6	594.8	595.6	0.659
z20	1.1	72.1	0.76	4160.0	0.238	0.096637	(.12)	0.79663	(.13)	0.05979	(.06)	594.7	594.9	595.9	0.887
z21	0.8	107.9	0.80	6173.3	0.250	0.096701	(.06)	0.79716	(.09)	0.05979	(.06)	595.0	595.2	595.9	0.715
Dacitic ash, Hingham (WE7-1A)															
z22	1.4	4.2	0.57	267.0	0.178	0.100936	(.75)	0.84285	(1.11)	0.06056	(.77)	619.9	620.7	623.7	0.725
z23	0.5	40.6	0.65	2376.6	0.203	0.097790	(.11)	0.80972	(.16)	0.06005	(.11)	601.4	602.3	605.5	0.700
z24	0.4	77.7	0.76	4382.6	0.244	0.097109	(.08)	0.80857	(.15)	0.06039	(.12)	597.4	601.7	617.5	0.579
z25	1.0	29.2	0.52	1765.0	0.164	0.097149	(.28)	0.80297	(.30)	0.05995	(.10)	597.7	598.5	601.6	0.939
z26	1.1	20.3	0.92	1123.4	0.287	0.096980	(.38)	0.79985	(.41)	0.05982	(.14)	596.7	596.7	597.0	0.941
z27	1.0	14.4	0.83	817.4	0.259	0.096908	(.56)	0.79859	(.62)	0.05977	(.25)	596.3	596.0	595.1	0.915
z28	0.9	17.6	0.90	981.8	0.278	0.096815	(.20)	0.79714	(.25)	0.05972	(.15)	595.7	595.2	593.3	0.812
z29	2.4	8.9	0.66	534.2	0.207	0.096623	(.36)	0.79663	(.43)	0.05980	(.22)	594.6	594.9	596.2	0.856

Notes: Corr. coef.—correlation coefficient. Age calculations are based on the decay constants of Steiger and Jäger (1977).
†All analyses are single zircon grains. Annealed and chemically treated analyses are underlined.
‡Pb_c is total common Pb in analysis. Pb* is radiogenic Pb concentration.
§Measured ratio corrected for spike and fractionation only.
#Radiogenic Pb ratio.
††Corrected for fractionation, spike, blank, and initial common Pb. Mass fractionation correction of 0.25%/amu ± 0.04%/amu (atomic mass unit) was applied to single-collector Daly analyses. Total procedural blank averaged 1.0 pg for Pb and <0.1 pg for U. Blank isotopic composition: $^{206}Pb/^{204}Pb = 18.27 \pm 0.1$; $^{207}Pb/^{204}Pb = 15.59 \pm 0.1$; $^{208}Pb/^{204}Pb = 38.12 \pm 0.1$.

Fig. 1; detailed mapping by Chute, 1966, 1969; Kaye, 1980). The geometry of these folds, however, differs considerably from the open form and gentle northeast plunge of folds found in most of the Boston Basin (Morell et al., 2004). The gentle folding is currently known only in rocks that are 490 Ma or older (Thompson et al., 2003), thus suggesting the possibility of older Paleozoic deformation as well.

U-Pb GEOCHRONOLOGY

New U-Pb zircon dates have been obtained from both the Lynn Volcanic Complex (sample MT95-1) and the Mattapan Volcanic Complex (samples MT01-28, MT-KK10, and WE7-1A). The composition and setting of each of the four samples, geochronological results, and their interpretations are discussed in the following sections. Major and trace element geochemical analyses of the rocks are listed in Table DR1 (see footnote 1), and U-Pb isotopic data appear in Table 1.

All analyses are from single zircon grains prepared and analyzed by the isotope dilution and thermal ionization mass spectrometry (ID-TIMS) method at the Geochronology Laboratory at the Massachusetts Institute of Technology, following the analytical procedures described in Appendix 1. The U-Pb isotopic dates and the associated uncertainties are calculated using the error propagation algorithm of Ludwig (1980). The final uncertainties reported for each of the samples incorporate both the internal (analytical) and external (systematic) sources of error. The latter includes the U-Pb tracer calibration error as well as the U decay constant errors of Jaffey et al. (1971). The incorporation of systematic errors in the calculated dates is necessary when results from different laboratories and/or different isotopic systems (e.g., U-Pb versus $^{40}Ar/^{39}Ar$) are compared (e.g., Schoene et al., 2006). Details of calculated age uncertainties are discussed in Appendix 1.

In general, when closed system behavior of the U-Pb system is inferred from a tight cluster of zircon analyses from a sample, the weighted mean $^{206}Pb/^{238}U$ date provides the most reliable estimate for the zircon crystallization age. However, in cases in which persistent Pb loss cannot be effectively eliminated by zircon pretreatment techniques (see Appendix 1), anomalously young Pb/U dates may result. If Pb loss is inferred to have occurred in geologically recent time, the weighted mean $^{207}Pb/^{206}Pb$ date provides a more accurate age estimate. In the case of ancient Pb loss, the only reliable age constraint may be obtained from the upper concordia intercept date.

Sample MT95-1: Rhyolite Porphyry (Saugus)

Rhyolite porphyry from Castle Hill, Saugus, Massachusetts (BOS18 in Fig. 1; analysis 3 in Table DR1, see footnote 1), represents a shallow intrusive or subvolcanic phase of the Lynn Volcanic Complex. The porphyry contains albite phenocrysts in a granophyric groundmass of albite, K-feldspar, and interstitial quartz with accessory allanite, apatite, ilmenite, and zircon. Four zircons, including three pretreated by chemical abrasion (z3, z5, and z6 in Table 1; see discussion of CA-TIMS in Appendix 1) and one pretreated by air abrasion (z4), yield overlapping analyses with a weighted mean $^{206}Pb/^{238}U$ date of 595.8 ± 1.2 Ma and an MSWD (mean square of weighted deviates) of 0.63 (Fig. 2A). Assuming that Pb loss is minimal or absent, this date is interpreted as the crystallization age of the rhyolite porphyry. Slightly younger Pb/U dates from air-abraded grains z8 and z9 probably reflect Pb loss because air abrasion is generally less effective than chemical abrasion in removing high U domains where Pb loss is most likely to occur. Two other analyses (z1 and z2) are distinctly older and have lower Th/U ratios than the others and are interpreted as inherited or xenocrystic zircons.

Sample MT01-28: Rhyolite Porphyry (Newton)

Rhyolite porphyry (analysis 4 in Table DR1; see footnote 1) at Nahanton Road, Newton, Massachusetts, in the center of the Boston Basin (BOS 3 in Fig. 1) intrudes a stratified sequence of

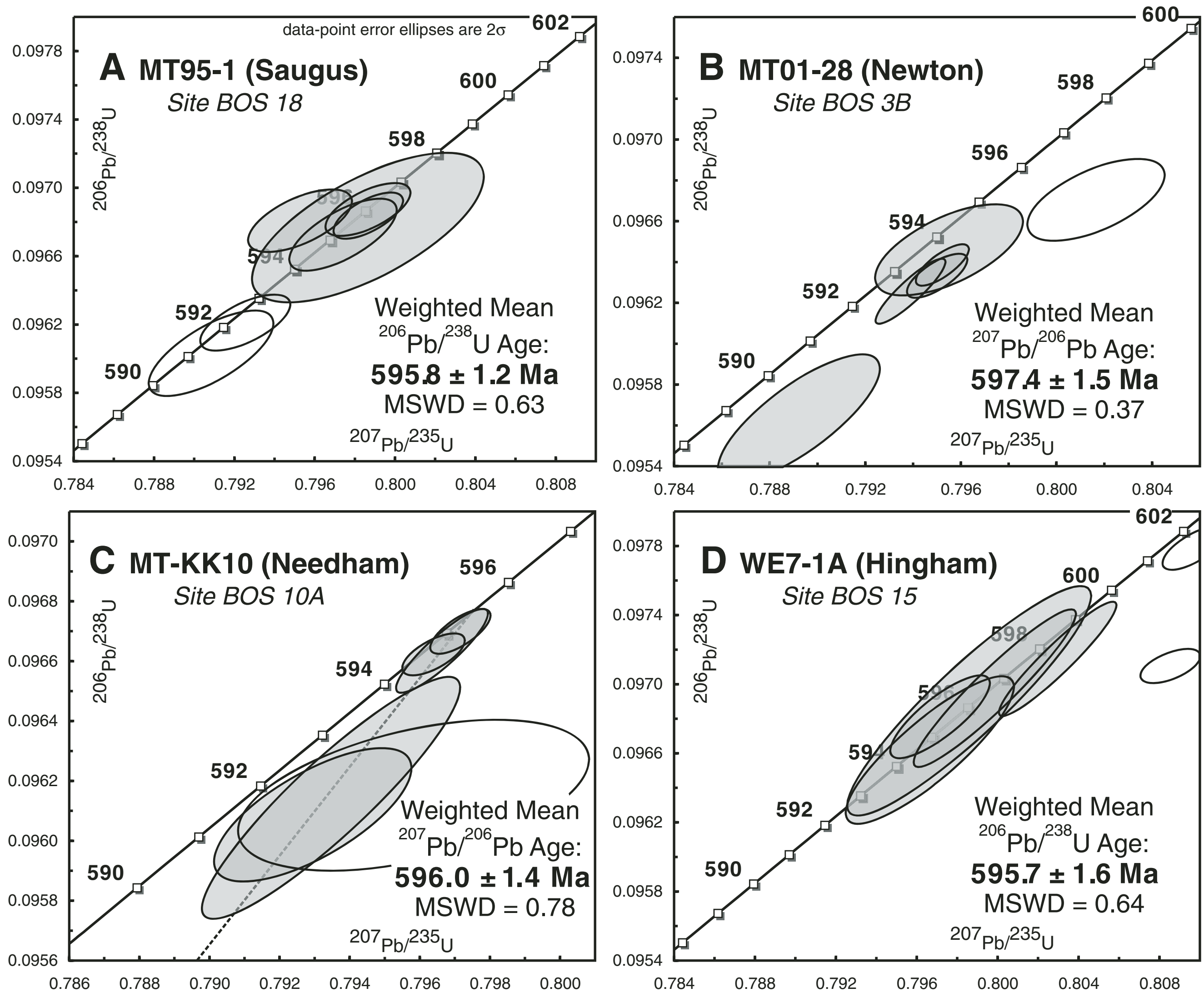

Figure 2. U-Pb concordia plots for Lynn-Mattapan samples from numbered paleomagnetic sites shown in Figure 1. Error ellipses represent 2σ analytical uncertainties that correspond to individual zircon analyses. Ellipses are shaded for data points used in age calculation. Isotopic data are listed in Table 1. Error calculations are discussed in Appendix 1.

dark-greenish-gray andesitic flows (represented by analysis 5 in Table DR1) and volcaniclastic interbeds. The sequence is folded about the same northeast-trending, gently northeast-plunging axis documented throughout much of the central part of the basin where the Boston Bay Group is not underlain by granitic basement. The porphyry is composed of albite and quartz phenocrysts surrounded by a patchy groundmass of albite and quartz with secondary muscovite and titanite. Accessory minerals include apatite, titanium-bearing iron oxide, and zircon. U-Pb analyses of five single zircon grains (z10, z11, z12, z14, z15 in Table 1 and Fig. 2B) yield a weighted mean $^{207}Pb/^{206}Pb$ date of 597.4 ± 1.5 Ma (MSWD = 0.37). These results also establish a minimum age for the andesitic host rock.

Sample MT-KK10: Rhyolitic Ash-Flow Tuff (Needham)

Pyroclastic rhyolite from Needham, Massachusetts (BOS 10 in Fig. 1), was collected from part of the Mattapan Volcanic Complex previously designated as the High Rock Tuff (analysis 7 *in* Thompson and Hermes, 1990). The dated sample consists of quartz, K-feldspar, albite, and altered biotite phenocrysts studded through a cryptocrystalline, felsitic matrix. Sparse pumice clasts are devitrified to form irregular lenses of quartz and feldspar. Accessory minerals include apatite, magnetite, and zircon. Five out of six analyzed single zircons (z16, z17, z19, z20, z21 in Table 1 and Fig. 2C) yield a weighted mean $^{207}Pb/^{206}Pb$ date of 596.0 ± 1.4 Ma (MSWD = 0.78), which overlaps well within error with their upper concordia intercept date of 595.5 ± 0.8 Ma (MSWD = 0.17). This tuff and ~100 m of overlying andesite (analysis 6 in Table DR1; see footnote 1) dip to the southwest on the flank of a shallow intrusive dome of fine-grained granite (Kaye, 1980; Thompson and Hermes, 1990).

Sample WE7-1A: Dacitic Ash (Hingham)

Dacitic volcanic ash (analysis 7 in Table DR1; see footnote 1) forms discontinuous, laminated horizons associated with basaltic lava flows (analyses 8 and 9 in Table DR1) that dominate the Mattapan volcanic sequence at Worlds End in Hingham, Massachusetts (BOS15 in Fig. 1). These were submarine eruptions on the basis of complex contact relationships in which the ash drapes the flows in some places but elsewhere is disrupted by bursting pillows to become engulfed as breccia blocks in the basalt (Ault et al., 2004). The ash is altered to intergrown epidote, albite, ferroactinolite, calcite, and quartz, with accessory titanite, chromite, iron oxides, copper sulfides, and zircon. The $^{206}Pb/^{238}U$ dates of four single zircon analyses (z26, z27, z28, z29 in Table 1 and Fig. 2D) define a tight cluster with a weighted mean of 595.7 ± 1.6 Ma (MSWD = 0.64) that we interpret as the crystallization age of the dacite. Other analyzed grains (z22 through z25 in Table 1; z22 not shown in Fig. 2D) are interpreted as variably influenced by inheritance. Three of these analyses are <1% discordant (z22, z23, z25; discordance of 0.61%, 0.68%, and 0.65%, respectively), and their $^{206}Pb/^{238}U$ dates of 619.9 Ma, 601.4 Ma, and 597.7 Ma fall within the range of ages reported from granites and volcanic rocks elsewhere in the Boston area. Such grains are interpreted as detritus derived from unroofed granite and/or older volcanic sequences that are also represented by clasts in volcaniclastic breccias interbedded with the lava flows at Worlds End. Billings et al. (1939) documented hundreds of feet of relief on the surface of the Dedham Granite underlying these and similar strata extending eastward into Nantasket, Massachusetts. Subhorizontal, cross-bedded sandstones deposited directly on the unroofed granite at Worlds End rule out postdepositional deformation in this area, so we interpret the gentle dips of units higher in the section as primary features developed over topographic irregularities present during volcanism and sedimentation. Mafic dikes trend approximately east-west parallel to faults cutting the area (Billings et al., 1939) and thus appear to be younger than the Mattapan eruptions.

PALEOMAGNETIC INVESTIGATION

Paleomagnetic samples were collected at six locations (142 cores) from the Lynn and Mattapan volcanic complexes and cross-cutting dikes in the vicinity of Boston, Massachusetts (Fig. 1). An additional three sites (33 cores) were drilled in red siltstones of the Squantum Member of the Roxbury Conglomerate. Lynn-Mattapan samples, all with dates at ca. 595 Ma for purposes of this discussion, were taken from rocks over a broad region to average out secular variation and to evaluate the possibility of structural disruption. Previously summarized structural observations were used, where feasible, to conduct paleomagnetic tests for assessing possible remagnetization events. Paleomagnetic sampling and laboratory procedures are summarized in Appendix 2, and the results are discussed as follows.

Multiple Magnetization Directions

Rocks from the Lynn and Mattapan volcanic complexes and from the Squantum Member of the Roxbury Conglomerate display a complex record of magnetization, typically with more than one stable direction at each site as shown in the complete paleomagnetic data set (including statistical parameters) in Table 2. The patterns in these data are more easily perceived in Table 3, in which recurrent directions are listed in columns that represent four distinct magnetic components designated A, B, C, and D (present-day field). Components A, B, and C are never observed to coexist in the same sample, though at site BOS15G half of the samples exhibit an A component, and half a C component. The characteristics of each of these components are summarized as follows.

Component A comprises directions that are southeast directed and upward pointing at Lynn-Mattapan sites BOS3A, BOS3B, BOS10B, and BOS15A, as well as antipodal directions that are northwest directed and downward pointing at sites BOS3E, BOS14A, BOS15G, BOS18A, and BOS18B. Samples from sites BOS3A, BOS3B, BOS3E, and BOS15A lose their magnetization between 600 and 690 °C, indicating the magnetic carrier to be hematite. Unblocking temperatures below 590 °C at the other sites show that magnetite likewise contributes significantly to this component of magnetization. Typical demagnetization curves for samples from several of these sites appear in Figure 3. The very fine-grained andesite from site BOS3A yielded anomalously low inclinations in comparison with other Lynn-Mattapan sites. We believe that secular variation may not have been completely averaged out from this site because the rock cooled more quickly than the other, more massive flows sampled above this unit. Component A is also present at Squantum site BOS11B (Fig. 3H).

Component B is south directed and steeply downward pointing at sites BOS10A, BOS14B, and BOS15D, with unblocking temperatures generally below 580 °C signifying magnetite as the principal magnetic carrier (Fig. 4A).

Component C is south-southeast to south directed and gently downward pointing. At sites BOS15J and BOS20A, this magnetization disappears below 590 °C (Fig. 4B), but unblocking temperatures reach 680 °C at site BOS15G and at sites BOS11A and BOS11C. As with component A, both magnetite and hematite are carriers of this remanence. The south-trending and very gently upward-pointing direction from the mafic dike at site BOS15B is also included in this group.

Component D, with unblocking temperatures between 100 °C and 400 °C, is present at three Lynn-Mattapan sites and at three sites in the Squantum Member of the Roxbury Conglomerate. This north-directed, downward-pointing component is similar to the Earth's present-day field of 344°, 69°N. The northwest direction at

TABLE 2. PALEOMAGNETIC DATA FROM THE LYNN AND MATTAPAN VOLCANIC COMPLEXES AND THE SQUANTUM MEMBER OF THE ROXBURY CONGLOMERATE

Site no.	Rock type	Lat °N	Long °W	NRM x 10^{-2} A/m	$X \times 10^{-5}$ SI	*n*/*N*	Plunge	Bedding	Com	D	I	α95	*Plat*	VGP PPlat	VGP PPlon.	Structurally corrected D^t	Structurally corrected I^t	Structurally corrected α95	*Plat.^{t}*	VGP PPlat^t	VGP PPlon^t
Lynn and Mattapan volcanic complexes																					
BOS3A†	Andesite	42°18.005′	71°11.7′	1.230	13	7/8	19–58	300/27E	A	106.2	–33.3	3.8	*–18*	24	202	127.0	–35.4	3.8	*–20*	40	189
BOS3B†	Andesite	42°18.025′	71°11.71′	1.530	32	8/13	19–58	300/27E	A	102.1	–53.2	7.5	*–34*	30	219	144.2	–54.4	7.5	*–35*	61	196
BOS3E†	Rhyolite	42°18.077′	71°11.752′	0.434	16	6/9	19–58	300/27E	A	272.7	59.8	13.9	*41*	28	230	324.8	61.0	13.9	*42*	64	210
BOS10A	Rhyolite	42°16.513′	71°15.492′	0.395	16	9/10			B	148.0	66.1	8.1	*48*	–5	130						
BOS10B†	Andesite	42°16.083′	71°16.493′	0.577	28	8/13			A	153.1	–53.5	10.2	*–34*	67	186						
BOS10B	Andesite					5/13				195.5	–86.0	5.2	*–82*	50	292						
BOS14A†	Rhyodacite	42°13.043′	71°14.096′	23.450	715	7/7			A	313.4	55.2	5.4	*36*	54	204						
BOS14B	Rhyodacite	42°12.888′	71°13.955′	8.511	808	5/9			B	192.1	62.9	9.6	*44*	3	100						
BOS14B	Rhyodacite					7/9			D	351.2	68.7	7.4	*52*	78	261						
BOS15A†	Basalt	42°16.008′	70°52.265′	0.408	63	4/4			A	138.8	–67.6	1.9	*–50*	61	230						
BOS15A	Basalt					4/4				65.3	62.2	8.1	*44*	43	354						
BOS15B	Mafic dike	42°15.9′	71°52.1′	58.540	5466	9/9				201.7	–4.6	8.8	*–2*	46	077						
BOS15D	Basalt	42°15.997′	70°52.294′	0.197	51	6/12			B	173.9	57.0	6.2	*38*	10	114						
BOS15D	Basalt					9/12			D	2.6	69.4	9.1	*53*	79	298						
BOS15G†	Basalt	42°15.966′	71°52.120′	1.800	46	4/8			A	301.0	70.4	9.2	*54*	50	238						
BOS15G	Basalt					4/8			C	175.0	10.3	18.0	*5*	42	116						
BOS15H	Breccia	42°15.921′	70°52.291′	1.050	39	6/7				244.1	17.7	51.4									
BOS15J	Mafic dike	42°16′	70°52.2′	196	6841	5/5			C	159.3	16.7	3.9	*8*	36	135						
BOS18A†	Rhyolite	42°29.362′	71°2.747′	1.167	9	7/7			A	327.5	59.9	8.1	*41*	66	206						
BOS18B†	Rhyolite	42°29.362′	71°2.747′	3.560	393	8/8			A	326.8	52.2	8.9	*33*	62	190						
BOS20A	Rhyolite	42°26.962′	71°1.678′	3.128	49	6/13			C	163.7	21.9	10.2	*11*	35	129						
BOS20A	Rhyollite					10/13			D	316.4	67.7	6.1	*51*	59	230						
Lynn-Mattapan mean (*n* = 9 sites†)										306.0	58.0	10.5	*39*			319.9	57.0	7.4	*38*		
Lynn-Mattapan mean pole		PPlat	PPlon.	A95																	
(*N* = 9 VGPs)		60	206	8.4																	
Squantum Member of the Roxbury Conglomerate																					
BOS11A	Siltstone	42°18.193′	71°0.666′	0.280	14	8/10	12–222	44/40S	C	164.3	8.2	15.2	*4*	42	130	173.5	–33.2	15.2	*18*	65	124
BOS11A	Siltstone					7/10	12–222	44/40S	D	19.7	71.7	12.4	*56*	71	324	109.1	54.1	12.4	*35*	10	341
BOS11B	Siltstone	42°18.260′	71°0.757′	0.255	17	11/13	12–222	53/40S	A	118.9	–10.7	9.4	*–5*	25	183	109.0	–63.4	9.4	*45*	40	228
BOS11B	Siltstone					9/13	12–222	53/40S	D	11.5	73.2	8.8	*59*	72	308	118.7	42.0	8.9	*24*	3	162
BOS11C	Siltstone	42°18.298′	71°0.590′	0.315	15	10/10	12–222	53/40S	C	186.8	39.1	8.9	*22*	25	102	180.1	7.1	8.9	*4*	44	109
BOS11C	Siltstone					8/10	12–222	53/40S	P	336.0	71.8	4.8	*57*	69	250	136.7	67.4	4.8	*50*	10	315

Notes: Site coordinates were determined from handheld global positioning system Magellan receiver or place name geographic directory; site locations are shown in Figure 1. NRM—natural remanent magnetization; *X*—initial susceptibility; *n*/*N*—number of samples used for site mean calculation/total number of samples; Plunge—plunge of fold axis; Bedding—strike/dip; Com—magnetic component; D—site mean declination; I—site mean inclination; α95—semi-angle of the cone of 95% confidence about the site mean; *Plat*—paleolatitude; VGP—virtual geomagnetic pole in Northern Hemisphere; PPlat—paleopole latitude; PPlon—paleopole longitude; A95—radius of error circle at the 95% confidence level; positive values are in the Northern Hemisphere, and negative values are in the Southern Hemisphere. Present-day field: 344.5°, 69°N.

†Directions used to calculate the Lynn-Mattapan mean.

TABLE 3. UNBLOCKING TEMPERATURES AND MEAN DIRECTIONS OF PALEOMAGNETIC COMPONENTS IN THE SOUTHEASTERN NEW ENGLAND AVALON ZONE AROUND BOSTON, MASSACHUSETTS†

Site	Rock type	Component A		Component B		Component C		Component D		Other	
		Unblocking temperature	D, I‡	Unblocking temperature	D, I‡	Unblocking temperature	D, I‡	Unblocking temperature	D, I‡	Unblocking temperature	D, I‡
Lynn and Mattapan volcanic complexes											
BOS3A	Andesite	600–690 °C	127, –35								
BOS3B	Andesite	600–690 °C	144, –54								
BOS3E	Rhyolite	150–690 °C	325, 61								
BOS10A	Rhyolite			200–580 °C	148, 66						
BOS 10B	Andesite	400–690 °C	153, –54							300–700 °C	196, –86
BOS14A	Rhyodacite	400–590 °C	313, 55								
BOS14B	Rhyodacite			400–580 °C	192, 63			0–400 °C	351, 69		
BOS15A	Basalt	500–675 °C	139, –68							0–450 °C	065, 62
BOS15B	Basalt (dike)					490–600 °C	202, –5				
BOS15D	Basalt			100–620 °C	174, 57			0–380 °C	003, 69		
BOS15G	Basalt	0–580 °C	301, 70			580–680 °C	175, 10				
BOS15J	Basalt (dike)					460–590 °C	159, 17				
BOS18A	Rhyolite	100–590 °C	328, 60								
BOS18B	Rhyolite	100–590 °C	327, 52								
BOS20A	Rhyolite					380–570 °C	164, 22	0–380 °C	316, 68		
Squantum Member of the Roxbury Conglomerate											
BOS11A	Siltstone					200–680 °C	164, 08	0–400 °C	020, 72		
BOS11B	Siltstone	570–690 °C	112, –52					0–400 °C	012, 73		
BOS11C	Siltstone					400–690 °C	187, 39	0–400 °C	336, 72		

†Complete data set in Table 2.
‡D, I—declination and inclination in degrees.

site BOS20A is grouped with component D on the basis of its unblocking behavior (<400 °C) and low coercivity (<10 mT).

Measurements of samples from sites BOS10B and BOS15A, listed in the right-hand column of Table 3, do not match any of the recurrent directions and remain unexplained.

Available microprobe data from paleomagnetically sampled units confirm the presence of hematite and magnetite as expected from the demagnetization behavior just described but reveal no petrographic patterns that establish the relative ages of the various components. The dual polarity of component A, however, argues that this magnetization is likely to have been acquired close to the time of eruption by deuteric oxidation above the Curie temperature in the cooling lavas. Components B and C are interpreted as younger chemical rather than thermal remagnetizations, because the nonmagnetic mineral assemblages in rocks throughout the study area reflect only mild heating under lower greenschist facies conditions. Fluid migration necessary to produce such chemical remagnetization seems plausible in the context of regionally documented Paleozoic events that are discussed in a later section.

Paleomagnetic Tests

Field tests were conducted wherever possible to determine whether any of the multiple Lynn-Mattapan and Squantum magnetizations might represent primary Neoproterozoic magnetic remanence. Few structural corrections are required for these assessments, because Lynn and Mattapan volcanic rocks were generally protected against later deformation by their position directly above the massive Dedham Granite. This is particularly clear at Worlds End (BOS15 in Fig. 1), where horizontal sandstone resting directly on unroofed granite has already been described. Elsewhere, the volcanic rocks show no cleavage or any other textural evidence for tectonic deformation. Even flattened, steeply aligned pumice clasts in ash-flow tuff at Twin Pine Hill (BOS14 in Fig. 1) can be satisfactorily interpreted to be primary structures like those developed in the Eocene Wall Mountain Tuff as it erupted against the walls of an ancient paleovalley (Chapin and Lowell, 1979). The one exception to this regional stability is the Nahanton Road locality (BOS3 in Fig. 1), which lies within the Boston Basin where granitic basement is absent or at least far below the volcanic section. Here, andesite flows interbedded with conglomerate and intruded by rhyolite porphyry dip moderately to the northeast, consistent with attitudes on the north limbs of folds that affect the Roxbury Conglomerate and Cambridge Argillite in other parts of the basin. The A components at sites BOS3A, BOS3B, and BOS3E have been unplunged and untilted using the structural data in Table 2, and compared with uncorrected A directions at six other Lynn-Mattapan sites (Table 3 and Fig. 5). Results from these nine sites pass the fold test of Watson and Enkin (1993), because directions show the best clustering at nearly 100% unfolding. Red siltstones at Squantum (sites BOS11A, BOS11B, BOS11C) have also been corrected for bedding tilt and plunge (Table 2), though a fold test is not possible because all sampled sites are in the same south-dipping sequence. It is worth noting that C magnetic components are recognized in the structurally uncorrected beds at Squantum, indicating that tilting predates the acquisition of this remanence.

Reversals tests were possible at Nahanton Road (BOS3B and BOS3E) and at Worlds End (BOS15A and BOS15G). Each pair of sites at both locations shows antipodal directions indicative of normal and reverse polarities. The critical angle at Nahanton Road is 13.9°, a positive reversals test with an R_c classification, according to McFadden and McElhinny (1990), because the critical angle lies between 10° and 20°. The Worlds End sites pass a reversals test with an R_b classification (9.9° critical angle falls between 5° and 10°).

A conglomerate test was attempted at Worlds End. Site BOS15H consists of seven basaltic clasts in volcaniclastic breccia overlying the basaltic flow represented by BOS15G. Six of these clasts contain only a high temperature component (between 600 °C and 680 °C), indicating

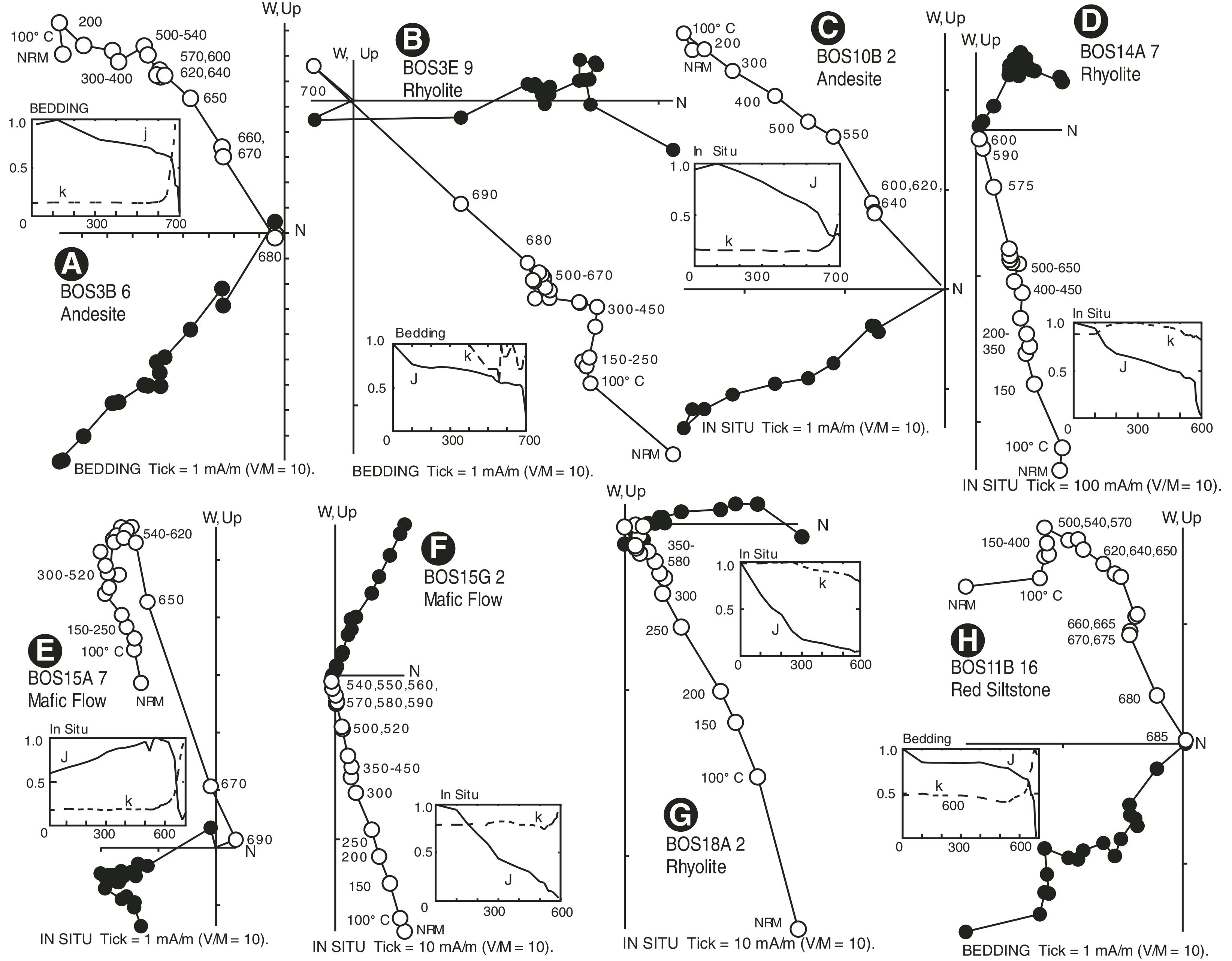

Figure 3. Orthogonal projection of vector endpoint diagrams, showing demagnetization behavior of samples containing A components. Open circles (solid circles) are projections on the vertical (horizontal) planes at the indicated levels of AF (mT, milliTesla) or thermal (°C) demagnetization. Normalized intensity (J/Jo) plots and susceptibility (k) vs. temperature plots are shown for lithologies for which thermal demagnetization was used. Numbered sample sites are shown in Figure 1. NRM—natural remanent magnetization.

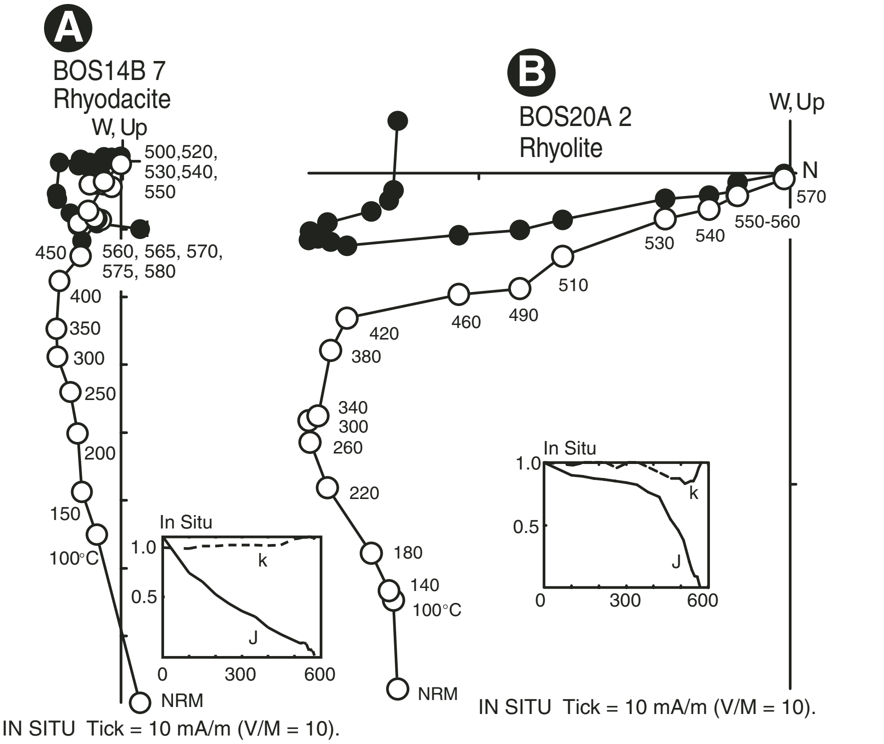

Figure 4. Orthogonal projection of vector endpoint diagrams, showing demagnetization behavior of samples containing B and C components. Open circles (solid circles) are projections on the vertical (horizontal) planes at the indicated levels of AF (mT, milliTesla) or thermal (°C) demagnetization. Normalized intensity (J/Jo) plots and susceptibility (k) vs. temperature plots are shown for lithologies for which thermal demagnetization was used. Numbered sample sites are shown in Figure 1. See Figure 3 caption for additional explanations.

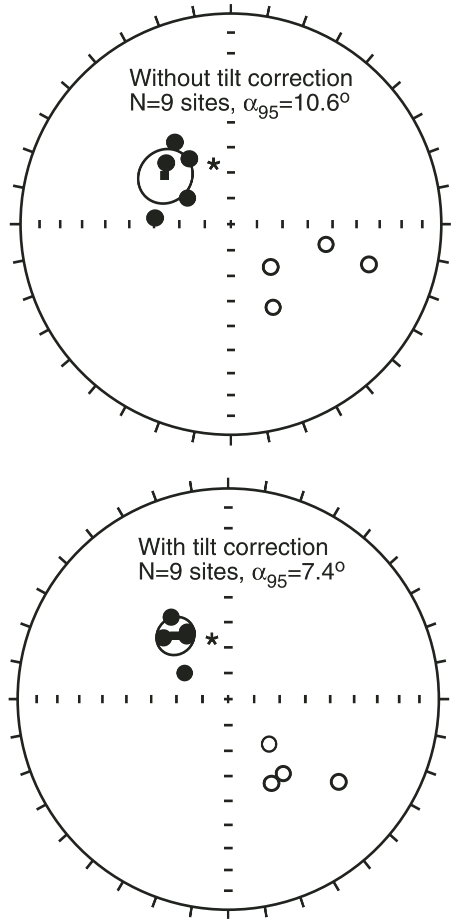

Figure 5. Equal-angle projections of site mean directions in the combined Lynn and Mattapan volcanic complexes, based on A component magnetizations at sites BOS3A, BOS3B, BOS3E, BOS10B, BOS14A, BOS15A, BOS15G, BOS18A, and BOS18B (Tables 2 and 3). Open (closed) symbols are on the upper (lower) hemisphere. Circle represents the α95 radius of 95% confidence for the directional mean. With tilt correction for sites BOS3B and BOS3E, the Lynn-Mattapan mean direction is D = 319.9°, I = 57.0° (α95 = 7.4°, *n* = 9 sites). Asterisk represents the present-day field (PDF) direction.

hematite as the magnetic carrier, in contrast to magnetite in the underlying flow. The directions from these clasts are almost random, with an R value (length of the resultant vector as defined by Watson, 1956) of 4.11 at the 95% confidence level. Although this is slightly above the critical R_c value of 3.85, the difference in magnetic carrier precludes meaningful comparison with the A direction in the BOS15G sample. The seventh clast contains a stable magnetization below 570 °C that is southeast and downward pointing, but this component does not overlap directions at the BOS15G site. For both of these reasons, the conglomerate test is inconclusive.

Two east-west–trending mafic dikes were also sampled at Worlds End to evaluate possible remagnetization effects in surrounding rocks. A ≥4-m-thick dike at the BOS15B site cuts the volcanic breccia described above (BOS15H). This dike contains a single component of magnetization between 490 °C and 600 °C that is south directed and very gently upward pointing, unlike directions obtained from any of the clasts in the volcanic breccia hosting the dike. A similar, though poorly grouped, direction is found in four of eight samples in the underlying flow (BOS15G in Table 3), suggesting possible overprinting in this unit. A 1–3-m-thick dike at site BOS15J contains a single component of magnetization below 590 °C that is southeast directed and downward pointing (component C in Table 3). This direction is not detected in the basaltic host rock at site BOS15D, ~30 m from the dike.

Overall, agreement among component A results obtained from variable primary magnetic carriers in different Lynn-Mattapan rock types that were either intruded or erupted in the greater Boston area during events closely clustered near 595 Ma constitutes a positive regional consistency test. Sampling also spans several different fault blocks across the study area, indicating that little local, vertical-axis rotation has been associated with postmagmatic deformation.

Neoproterozoic Mean Directions and Paleopoles

A mean direction has been calculated for the combined Lynn and Mattapan volcanic complexes on the basis of the A component of magnetization at nine sites in Tables 2 and 3. In these calculations, bedding is unplunged and untilted at Nahanton Road (BOS3A, BOS3B, BOS3E), but directions are uncorrected at the other sites, as described previously. The mean Lynn-Mattapan direction is D = 319.9°, I = 57.0° (α95 = 7.4°, *n* = 9 sites) (Fig. 5). The paleopole determined from virtual geomagnetic paleopoles at the nine sites is 206°E, 60°N, and the corresponding paleolatitude is 38° ± 8°. Based on the paleomagnetic tests outlined in the previous section, we believe that the mean Lynn-Mattapan direction represents a primary Neoproterozoic magnetization at ca. 595 Ma and that the mean paleopole is representative of the Avalon Zone in southeastern New England.

Directions broadly comparable to the Lynn-Mattapan mean have also been obtained at one of the three Squantum sites, BOS11B. Siltstone sampled at this site lies directly below diamictite that is less intensely fractured than siltstones elsewhere in the section. The tilt and plunge corrected site mean at BOS11B is D = 109.0°, I = –63.4°, $\alpha95$ = 9.4° (*n* = 11 samples). Although a fold test is not possible for the Squantum site, the uncorrected paleopole is not similar to known poles from Laurentia or Avalonia. We suggest that this result, too, may represent a primary Neoproterozoic direction acquired after 595 Ma. The virtual geomagnetic paleopole based on this direction is 228°E, 40°N.

Evidence for Younger Magnetizations

Lynn-Mattapan and Squantum results also include magnetizations that can be constrained as younger than Neoproterozoic. Component D (Tables 2 and 3) has already been noted as reflecting viscous overprinting from the Earth's present-day field. Evidence for post-Neoproterozoic ages of components B and C are discussed as follows.

The south-directed and downward-pointing B component found in Neoproterozoic volcanic rocks at sites BOS10A, BOS14B, and BOS15D (Tables 2 and 3) is also present as a secondary component in ca. 491 Ma syenite associated with the Nahant Gabbro on Boston's north shore (Fig. 1; Thompson et al., 2004). Component B must therefore represent remagnetization sometime after the syenite intruded in the Early Ordovician. The Southeastern New England Avalon Zone is dotted with middle Paleozoic alkalic plutons (Hermes and Zartman, 1992; Hepburn et al., 1993), including the Quincy Granite (Fig. 1), that could have generated fluids that resulted in chemomagnetic overprinting in this interval. Paleopoles based on B directions (Table 2) are similar to the pole reported for Middle Ordovician volcanic rocks at Dunn Point, Nova Scotia (Van der Voo and Johnson, 1985; Johnson and Van der Voo, 1990; age clarified as 460 Ma by Hamilton and Murphy, 2003), and to Devonian poles for Laurentia (Torsvik and Cocks, 2004).

A second possible Paleozoic direction is the southeast-directed and gently downward-pointing component C recognized at sites BOS11A, BOS11C, BOS15B, BOS15G, BOS15J, and BOS20A (Tables 2 and 3). This component is found in and around mafic dikes at Worlds End (BOS15B, BOS15G, and BOS15J), where hematite staining is common on joints and fractures. We suspect that individual cores have locally intersected such surfaces, so that some of the BOS15G samples exhibit the C component and some A component. At Squantum, component C is present in intensely fractured zones at the top and base of the section (samples BOS11A and BOS11C, respectively), but not in samples directly underlying the less fractured diamictite in between (BOS11B). This direction also occurs at site BOS20A closely adjoining the fault bounding the Boston Basin on the north (Fig. 1). All of these relationships are consistent with the origin of component C during chemical remagnetization linked with dike intrusion and associated fluid migration along regional faults and fractures. At least some of this activity took place in the late Paleozoic, because major faults cut formations as young as the Pennsylvanian strata of the Norfolk Basin (Fig. 1). A late Paleozoic overprinting is further supported by the similarity between paleopoles calculated from our C directions (Table 2) and mean Late Carboniferous to Early Permian paleopoles for Laurentia (Torsvik and Cocks, 2004).

Paleomagnetic Comparison with Other Avalonian Terranes

Lynn-Mattapan volcanic rocks and siltstones in the Squantum Member of the Roxbury Conglomerate are not the only sequences from Avalonian terranes that contain a diverse array of magnetizations. Paleomagnetic investigation in arc-related units in the type Avalon Zone of eastern Newfoundland, for example, reveals four magnetic remanence directions in porphyritic stocks and rhyolitic sills associated with volcano-sedimentary strata of the Harbour Main Group (Seguin and Lortie, 1986; ca. 606 Ma U-Pb zircon date later determined by Krogh et al., 1988). Four different directions were found in overlying basalts (Seguin and Giasson, 1987; Blue Hills Basalt of O'Brien et al., 2001) for which a maximum age is also provided by the 606 Ma zircon date. A similarly complex picture emerged from the Avalon terrane of southeastern Cape Breton Island at a time when ages of rocks in this coastal belt could only be estimated as 630–600 Ma by correlation with Rb-Sr–dated units in New Brunswick. Three magnetic components were reported from volcanogenic sediments of the Fourchu Group (Johnson and Van der Voo, 1986), and the associated "Fourchu Gabbro" yielded four distinct directions (Seguin et al., 1991). Remapping and U-Pb geochronology in this area (reviewed by Barr and White, 1996) now restrict the Fourchu Group, including some gabbro, to units dated at ca. 575 Ma by the comagmatic Capelin Cove pluton but assign most of the paleomagnetically sampled gabbro to the younger Main-à-Dieu Group. The common denominator among all of these paleomagnetic data is that remanence directions interpreted to represent the oldest magnetizations in the Newfoundland and Nova Scotia study areas give rise to paleopoles that agree remarkably well, given the age spread, with our 595 Ma Lynn-Mattapan pole at 206°E, 60°N (Table 4). As listed in the International Association of Geomagnetism and Aeronomy Global Paleomagnetic Database (http://dragon.ngu.no//), these include the Harbour Main C pole at 206°E, 48°N (Seguin and Lortie, 1986), the Fourchu Group A pole at 225°E, 56°N (Johnson and Van der Voo, 1986), and the Fourchu Gabbro B pole at 193°E, 63°N (Seguin et al., 1991).

Paleomagnetic data are also available for the 580–570 Ma Marystown Group in the Burin Peninsula, Newfoundland (McNamara et al., 2001). Although the ages of basaltic flows and clastic sediments are reasonably well constrained in this study, problems with vertical axis rotations prevented the calculation of paleopoles from tilt- and strike-corrected mean directions. The reported paleolatitude of 34° + 8°/–7°, however, overlaps values of 38° ± 8° inferred from the ca. 595 Ma Lynn-Mattapan directions. A slightly lower paleolatitude of 27° ± 8° has been obtained from the Caldecote Volcanic Formation in the Nuneaton inlier of Central England (Vizan et al., 2003). These strata are older than 602 Ma (U-Pb zircon date of Tucker and Pharaoh, 1991), the age of granophyric diorite that is interpreted to represent the final phase of arc magmatism in this eastern part of Avalonia.

PALEOGEOGRAPHIC IMPLICATIONS

Position of Avalonia with Respect to Gondwana

The consistency in predicted paleolatitude and the similarities among paleopoles from the Avalonian paleomagnetic data sets just reviewed argue strongly that Avalonian terranes occupied a midlatitude position in the period between ca. 600 Ma and 575 Ma. This leaves the larger paleomagnetic problem of relating these terranes to the Gondwanan margin. The first step in this reconstruction is to fix the position of Gondwana itself. This we have done by using the only two reasonably well constrained (i.e., $\alpha95 < 15$) West Gondwanan poles that date between 575 Ma and 615 Ma (±20 Ma from the 595 Ma Lynn-Mattapan paleopole). These poles are (1) the Bir Safsaf pole from the East Sahara craton of southwestern Egypt, based on seven granodiorite porphyry dikes dated at 586 ± 13 Ma (pole and K-Ar biotite date of

TABLE 4. PALEOMAGNETIC POLES FROM AVALONIA AND WEST GONDWANA

Location	Rock unit	Isotopic age[†]	PPLong[‡]	PPLat[‡]	A95[§]	Paleo-latitude
Avalonia						
Massachusetts, USA	Lynn and Mattapan volcanic complexes (A component)[#]	Ca. 595 Ma	206	60	7.4	38
Nova Scotia, Canada	Volcanogenic sediments, Fourchu Group (A component)	Ca. 575 Ma	225	56	5.0	44
Nova Scotia, Canada	Fourchu Gabbro (B component)	<575 Ma	196	63	6.4	34
Newfoundland, Canada	Rhyolite, Harbour Main Group (C component)	606 Ma	211	48	10.0	29
Newfoundland, Canada	Marystown Group	580–570 Ma	N.D.	N.D.	N.D.	34
Nuneaton, England	Caldecote Volcanic Formation	>603 Ma	N.D.	N.D.	N.D.	27
West Gondwana						
Egypt, Africa	Bir Safsaf granophyre dikes	Ca. 586 Ma	250	80	9.2	14
Brazil, South America	Campo Alegre volcanic rocks	Ca. 595 Ma	223	–57	9.0	23

[†]All dates except for Bir Safsaf based on U-Pb. Details in text.
[‡]PPLong and PPLat are, respectively, longitude and latitude of the paleopole.
[§]A95 is radius of error circle at the 95% confidence level, and only poles with A95s (or α95s) <15° have been included.
[#]This study; other poles, in descending order, from Johnson and Van der Voo (1986), Seguin et al. (1991), Seguin and Lortie (1986), McNamara et al. (2001), Vizan et al. (2003), Saradeth et al. (1989), D'Agrella-Filho and Pacca (1988).

Saradeth et al., 1989), and (2) the Campo Alegre pole from the Rio de la Plata craton of southeastern Brazil (D'Agrella-Filho and Pacca, 1988), derived from rhyolitic volcanic rocks for which the tightest U-Pb zircon constraint is 604 ± 5 Ma (Basei et al., 1998; Cordani et al., 1999). These two Gondwanan poles are nearly identical when Campo Alegre is rotated to Africa using the rotation parameters of Lawver and Scotese (1987). The overlapping pole positions provide support for the view that much of West Gondwana was broadly assembled by ca. 600 Ma (Pimentel et al., 1997; Alkmim et al., 2001; Cordani et al., 2001). Although parts of central West Gondwana were still undergoing high-grade metamorphism and shear zone deformation during the Cambrian (Schmitt et al., 2004; Trindade et al., 2006), we suggest that these events postdate major ocean closures during West Gondwana assembly and that they may not have involved *paleomagnetically* significant motion or rotation. This assumption is certainly less than ideal, but it avoids the comparably troublesome reliance on ambiguous high versus low latitude Laurentian poles (Pisarevsky et al., 2000; Meert and Van der Voo, 2001) as proxies for positioning Amazonia (recent examples in McNamara et al., 2001, and Murphy et al., 2004).

Gondwana straddles the equator in the reconstruction based on the Bir Safsaf and Campo Alegre poles but could be oriented with the current northern African margin in either the Northern or the Southern Hemisphere because of the inherent uncertainty over the polarity of these poles. Orienting Gondwana with northern Africa to the north of the equator at ca. 595 Ma, however, requires an average drift velocity of at least 13 cm/yr for more than a hundred million years as northern Africa moved to its accepted position near the South Pole in Late Cambrian time (Grunow and Encarnacion, 2000). We have shown northern Africa in the Southern Hemisphere (Fig. 6) because this interpretation halves the average drift velocity in the 595 Ma to 495 Ma interval, but the Northern Hemisphere location is also possible if there was rapid motion in the Early to Middle Cambrian (Kirschvink et al., 1997).

Avalonia, like the African margin of Gondwana, can be situated either north or south of

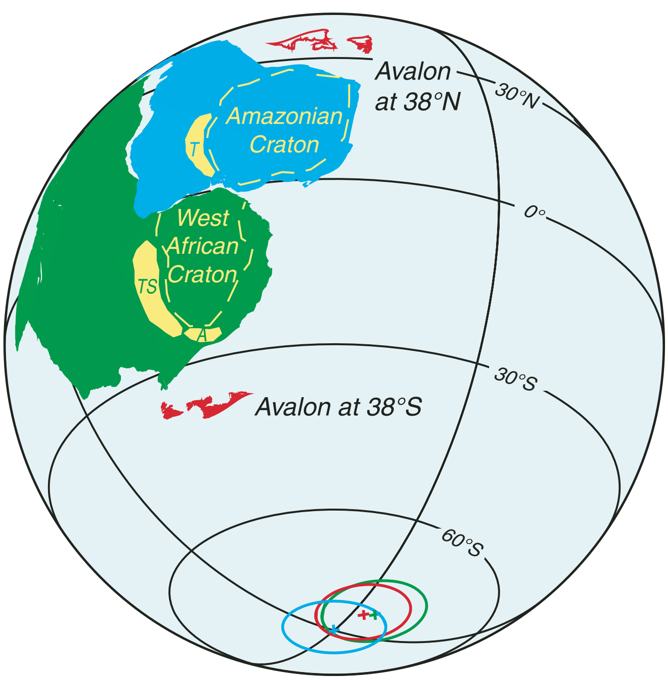

Figure 6. Plate reconstructions of Avalonia and West Gondwana at ca. 595 Ma, based on the mean poles listed in Table 4. The geographic South Pole is centered on the Brazilian Campo Alegre reference pole with its A95 circle (blue). Also shown are poles and A95 circles from the combined Lynn and Mattapan volcanic complexes as determined in this study (red), and Bir Safsaf granophyre dikes from SW Egypt (green). The preferred position of Avalonia at ~38°S lat adjoining the present-day northern margin of West Africa is shown in solid red, but a position at ~38°N lat in the bight of the South American coastline is also possible (red outline). Nd isotopic compositions discussed in the text come from rock sequences in the Tocantins Province of Brazil (T), trans-Saharan localities in Algeria and Mali (TS), and the Anti-Atlas orogen of Morocco (A). Peri-Gondwanan terranes representing Ganderia are not included in these reconstructions.

the equator and be consistent with the Lynn-Mattapan pole at ca. 595 Ma. If the Lynn-Mattapan paleolatitude is ~38°S, Avalonia would border the West African craton (solid red in Fig. 6). A second paleomagnetically permissible niche for Avalonia lies in the bight of the Amazonian craton at a paleolatitude of ~38°N (red outline in Fig. 6).

We view the African alternative as more plausible for two reasons. First, the reconstruction based on the 580–570 Ma Marystown Group in Newfoundland (McNamara et al., 2001) shows Avalonia in the same relative position with respect to the West African craton (even though the northern Gondwanan margin appears at a higher southerly paleolatitude, because Laurentian poles are used as proxies to constrain West Gondwana). Second, the paleomagnetically determined Amazonian position adjacent to the Pampean and Arequipa-Antofalla cratonic fragments of western South America lies far from the northwest Amazonian location commonly suggested for Avalonia on the basis of geological arguments (Nance and Murphy, 1994, 1996; van Staal et al., 1996; Murphy et al., 2002, 2004). On both counts, it becomes essential to reconsider whether geological evidence might be reconciled with the Avalonian–West African linkage emphasized in Figure 6.

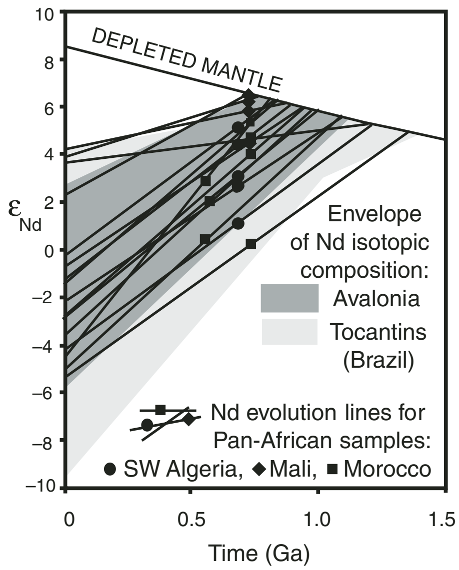

Figure 7. Nd-isotope-evolution diagram comparing isotopic compositions from Avalonia, the Tocantins Province of central Brazil, and samples from Pan-African belts in Morocco, Algeria, and Mali. Avalonian envelope of Nd isotopic compositions after Nance and Murphy (1996), based on data from Fryer et al. (1992), Barr and Hegner (1992), Whalen et al. (1994), Kerr et al. (1995), and Murphy et al. (1996). Tocantins envelope based on data of Pimentel and Fuck (1992) and Pimentel et al. (1997). Nd evolution lines for African samples based on data from Thomas et al. (2002), Caby et al. (1989), and Dostal et al. (2002). Depleted mantle curve from DePaolo (1981).

Geological Considerations

One geological requirement for any continental mass that may have been originally connected to Avalonia is the presence of juvenile ca.1 Ga basement (Murphy et al., 2002, 2004) that could have given rise to initial ε_{Nd} values between –0.5 and +5.0 for ca. 630 Ma to 550 Ma felsic igneous rocks of Avalonian terranes in Newfoundland, New Brunswick, and Nova Scotia. These values fall within the dark shaded area in Figure 7 (after Nance and Murphy, 1996). Source rocks that could have generated these ε_{Nd} values were first recognized among 950–900 Ma calc-alkaline granitoid orthogneisses and younger metarhyolites of the Tocantins Province in central Brazil (Fig. 6; Nance and Murphy, 1994, 1996), a Neoproterozoic orogenic belt that records the amalgamation of the São Francisco and Amazonian cratons during the Brasiliano orogenesis, which was associated with formation of West Gondwana (Pimentel and Fuck, 1992; Pimentel et al., 1997). Samples from this belt (light shading in Fig. 7) substantially overlap Avalonian Nd isotopic compositions, but some of them extrapolate to older intersections (i.e., depleted mantle model ages) on the depleted mantle curve of DePaolo (1981).

Nd isotopic parallels with Tocantins rocks, however, do not establish a direct spatial or geographic connection with Avalonia (McNamara et al., 2001). In view of the paleomagnetic interpretation in this paper, it is significant that comparable Nd isotopic signatures are now also documented in the Pan-African Anti-Atlas orogen, which was active along the northern margin of the West African craton during Gondwana assembly. In particular, rocks in the Sirwa window (Morocco) record island-arc–related subduction at ca. 740 Ma, followed by arc-continent collision at ca. 660 Ma and late to postorogenic sedimentation and magmatism between 615 Ma and 580 Ma (Thomas et al., 2002). Samples from the 743 Ma Bleida Group (SHRIMP [sensitive high-resolution ion microprobe] date of Thomas et al., 2002) show positive initial ε_{Nd} values up to +7.3 that are interpreted to indicate only minor crustal material as protolith. Values from Ouarzazate Group rhyolites and coeval granites (SHRIMP dates of 577 Ma to 559 Ma) show slightly more constricted initial ranges (ε_{Nd} from +0.37 to +2.87). Nd isotopic evolution lines from the Anti-Atlas samples (black lines with $\varepsilon_{Nd,\,t}$ marked by squares in Fig. 7) are largely confined within the envelope of Avalonian Nd isotopic compositions.

Nd isotopic evolution lines are also plotted in Figure 7 for igneous and metasedimentary units in the Trans-Saharan belt marking the suture between the West African craton and the Saharan paleocontinent on the east. One Trans-Saharan location is in the Sebkha el Melah inlier of southwestern Algeria, where a thick marginal marine sequence deposited between 720 Ma and 635 Ma (U-Pb zircon dates of Caby and Andreopoulos-Renaud, 1989, and Caby et al., 1989) includes volcanogenic sedimentary rocks intercalated with subduction-related volcanic flows (Dostal et al., 2002). Five volcanic samples from this sequence yield initial ε_{Nd} values between +1 and +5 at 680 Ma. Farther south in the Trans-Saharan belt of Mali, positive initial ε_{Nd} values (+4.4 to +6.8) are likewise reported for 730 Ma subduction-related metadiorites and metagraywackes (Caby et al., 1989). These examples, together with the Anti-Atlas example above, suggest that African crustal materials much closer to our paleomagnetically located Avalonia also represent isotopically suitable basement material.

Avalonia also must have originated in some proximity to source rocks that could have supplied ubiquitous 1.3 Ga to 0.9 Ga detrital zircons found in stratified units from Nova Scotia, New Brunswick, and southeastern New England (Bevier et al., 1990; Karabinos and Gromet, 1993; Magee and Gromet, 1996; Keppie et al., 1998; Thompson and Bowring, 2000; Barr et al., 2003). Possible provenance options for such zircons include Grenvillian belts in eastern Laurentia and Baltica, but belts of similar age that border the Amazonian craton (Teixeira et al., 1989) are commonly construed as more favorable sources in terms of peri-Gondwanan paleogeography. The only peri-Gondwanan position that has always been ruled out (following Hoffman, 1991) for lack of suitable Mesoproterozoic sources, ironically, is the position along the West African margin suggested both by this study and by McNamara et al. (2001).

One possible solution to the provenance difficulty might be to derive observed 1.3 Ga to 0.9 Ga detritus not from the nearest craton but longitudinally from other terranes along the Gondwanan margin or even from a terrane separating Avalonia from West Gondwana. Potentially suitable candidates are middle American terranes including Ouaxaquia (eastern Mexico), the Maya terrane (Yucatan Peninsula), and the Chortis block (Honduras and Nicaragua).

Ouaxaquia, for example, contains a diverse sequence of igneous and metamorphic basement rocks with U-Pb zircon dates between ca. 1.1 Ga and 0.9 Ga (Keppie and Ortega-Gutiérrez, 1995; Keppie et al., 2001; Ortega-Obregón et al., 2004). Circa 1.2 Ga orthogneisses in the Maya terrane were affected by granulite facies metamorphism at 990–975 Ma (U-Pb dates of Weber and Köhler, 1999; Ruiz et al., 1999). All of these terranes have been shown in various starting positions adjacent to northwestern Amazonia (Keppie et al., 1998, 2001; Murphy et al., 2002, 2004). It has even been suggested (Murphy et al., 2002) that these blocks could have extended the Amazonian margin 500–1000 km northward to approximately the same paleolatitude inferred for Avalonia both in this study and by McNamara et al. (2001).

A second aspect of Avalonian detrital zircon suites is also worth mentioning in light of the paleomagnetic evidence for an origin near the West African craton. An *expected* detrital zircon component of strata deposited in this setting would be Paleoproterozoic grains in the ca. 2.27–2.05 Ga interval marking the juvenile crust-forming events loosely known as the Eburnean orogeny (Hirdes and Davis, 2002, and included references). Zircons of this age are rare in Avalonian-cycle sandstones (Barr et al., 2003), but they have been identified in quartzite of the Blackstone Group (2.17 Ga and 2.06 Ga evaporation analyses of Magee and Gromet, 1996), which predates Avalonian arc magmatism in southeastern New England. High concentrations of detrital zircon ages ca. 2.0 Ga are also reported from quartzite clasts in conglomerates from the Caledonia and Mira terranes in New Brunswick and Nova Scotia, respectively (Barr et al., 2003). It appears from these examples that older Avalonian sedimentary sequences could have been supplied in part by source areas of Eburnean age but that transport patterns changed with the onset of Avalonian tectonism so that ca. 2.0 Ga Paleoproterozoic zircons are present only locally as recycled components.

CONCLUSION

The Late Neoproterozoic Lynn and Mattapan volcanic complexes around Boston, Massachusetts, record arc magmatism in the Avalonian terrane of southeastern New England. Paleomagnetic results from nine Lynn-Mattapan sites with differing lithology and ferromagnetic mineralogy reveal a regionally consistent A component of magnetization that passes both reversal and fold tests. These results indicate that the Lynn-Mattapan mean direction of D = 319.9°, I = 57.0° ($\alpha95$ = 7.4°, n = 9 sites) represents primary Neoproterozoic magnetization in rocks for which four new ID-TIMS U-Pb zircon ages determined in this study all cluster near 595 Ma. The Lynn-Mattapan mean direction gives rise to a mean paleopole of 206°E, 60°N that agrees with the best constrained Neoproterozoic poles from Avalonian terranes in Newfoundland and Nova Scotia, and all of these poles suggest that Avalonia occupied a midlatitude position between ca. 600 Ma and 575 Ma. A similar conclusion is reported from Nuneaton, England, representing the eastern end of the Avalonian lithotectonic belt.

The Lynn-Mattapan pole allows Avalonia to be located along the Gondwanan margin, which, in this study, has been reconstructed using reasonably well-constrained West Gondwanan poles from Campo Alegre (Brazil) and Bir Safsaf (Egypt). Northern Africa is placed in the Southern Hemisphere in the reconstruction to achieve reasonable drift velocities between 595 Ma and 495 Ma, at the end of which time northern Africa lay near the South Pole. Two midlatitude, peri-Gondwanan positions for Avalonia are possible within this framework: either adjacent to northern Africa at lat 38°S, or in the bight of the western Amazonian margin at lat 38°N. We view the African alternative as more plausible, because a similar position was deduced by McNamara et al. (2001) using other methods. Geological evidence, including Sm/Nd isotopic signatures and detrital zircon suites, can be interpreted to support this reconstruction.

Stable B and C magnetic components in Lynn-Mattapan rocks record directions that suggest, respectively, Middle Ordovician to Late Devonian and Late Carboniferous to Early Permian magnetizations. These magnetic components should be further examined for clues they may provide about the post-Avalonian tectonic history of the Southeastern New England Avalon Zone.

APPENDIX 1. ANALYTICAL METHODS FOR U-PB GEOCHRONOLOGY

Zircon was separated from bulk rock samples by standard crushing, heavy liquid, and magnetic separation techniques, and was subsequently handpicked using a binocular microscope, with selection based on clarity and crystal morphology. All grains were pretreated to minimize the effects of Pb loss, but the pretreatment protocol evolved significantly during the course of this study. For most of the analyses (which were performed early in the study), removal of the outer parts of grains was accomplished by mechanical abrasion with pyrite inside air-abrasion vessels (Krogh, 1982). The last grains to be analyzed (analyses z2, z3, z5, z6, and z7 in Table 1), however, were treated by thermal annealing and chemical leaching (chemical abrasion–thermal ionization mass spectrometry, or CA-TIMS technique: Mattinson, 2005) designed to preferentially remove the high-U parts of the zircon crystal that are most susceptible to Pb loss. Zircon grains are first annealed at 900 °C for 60 h and subsequently leached in 29M HF at 180 °C for 12 h. The partially dissolved sample is then fluxed successively with hot 4N HNO_3 and 6N HCl in an ultrasonic bath and thoroughly rinsed with ultra-pure water in between. Air-abraded zircons are cleaned in a similar fashion by fluxing in warm 4N HNO_3 to remove surface contaminants. Both air-abraded and annealed-leached zircons were spiked with a mixed ^{205}Pb-^{233}U-^{235}U tracer solution and dissolved completely in 29M HF inside high-pressure Parr® vessels at 220 °C for 48–60 h.

Dissolved Pb and U were chemically separated using a miniaturized HCl-based ion-exchange chromatography procedure modified after Krogh (1973), using 50 μL columns of AG 1 × 8 anion-exchange resin. Both Pb and U were loaded with a silica gel–H_3PO_4 emitter solution on single degassed Re filaments, and their isotopic compositions were measured on the VG Sector 54 multi-collector thermal ionization mass spectrometer at the Massachusetts Institute of Technology. Lead isotopes were measured in a peak-switching mode by ion counting using a Daly photomultiplier detector with a ^{206}Pb ion beam intensity of 0.5–2.0 × 10^{-13} A usually maintained in the course of data acquisition. Uranium isotopes were measured as oxide ions on three Faraday detectors in a static mode with an average $^{235}U^{16}O_2^+$ ion-beam intensity of 9.0 × 10^{-13} A.

Measured isotopic ratios were corrected for mass-dependent isotope fractionation in the mass spectrometer, as well as for U and Pb contributions from the spike, and laboratory blanks. Details of fractionation and blank corrections are given in Table 1. The U-Pb data reduction, age calculation, and error propagation follow the algorithm of Ludwig (1980) and the program Isoplot (Ludwig, 1991; version 3.14, 2004) using the decay constants of Jaffey et al. (1971). All U-Pb dates are reported at 95% confidence levels and are plotted on conventional concordia plots (Figs. 2A–D).

During the time that the U-Pb data presented in this study were acquired, it has become clear that high-precision analyses of zircon that result in statistically equivalent data commonly exhibit a slight age discordance manifested by $^{207}Pb/^{206}Pb$ dates that are systematically older than the corresponding Pb/U dates by a minimum of 0.2%. This discordance is likely due to imprecision in one or both of the U decay constants (Mattinson, 2000; Schoene et al., 2006). In many studies of lower Paleozoic and older zircons plagued by Pb loss that is inferred to have occurred in geologically recent times, $^{207}Pb/^{206}Pb$ dates have been considered the best estimate of the crystallization age of a discordant population. In this case, uncertainties in the decay constants can be ignored if the dates are not compared with dates calculated using other chronometers. Now, discordance related to radiation damage and Pb loss can often be effectively eliminated through the chemical abrasion technique outlined at the beginning of this section. A data set for a single population of zircons for which Pb loss has been eliminated is manifested by a tight cluster of data, termed *equivalent* by Ludwig (1998) in which all scatter can be accounted for by analytical uncertainty. In these cases the weighted mean $^{206}Pb/^{238}U$ date is generally the most precise and accurate. For some samples, equivalent data sets are not obtainable, and we instead rely on either the $^{207}Pb/^{206}Pb$ or the upper concordia intercept date, depending on the data. Detailed U-Pb date errors are reported as follows: ±X/Y/Z, where X is the internal uncertainty in absence of all systematic error (tracer calibration and decay constants), Y includes the tracer calibration error (using a conservative estimate of the 2σ standard deviation of the Pb/U ratio in the tracer = 0.05%), and Z includes the tracer calibration and decay constant errors of Jaffey et al. (1971). For $^{207}Pb/^{206}Pb$ dates, tracer errors are negligible, and Y is

TABLE A1. COMPLETE U-Pb DATE ERRORS FOR LYNN-MATTAPAN VOLCANIC ROCKS

Sample no. / *(n)*	Date calculated from	Weighted mean age ± 2σ error [MSWD]
MT95-1 / (4)	$^{206}Pb/^{238}U$	595.81 ± 0.42/0.50/1.2 Ma [0.69]
MT01-28 / (5)	$^{207}Pb/^{206}Pb$	597.41 ± 0.89/1.55 Ma [0.37]
MT-KK10 / (5)	$^{207}Pb/^{206}Pb$	595.97 ± 0.74/1.4 Ma [0.30]
WE7-1A / (4)	$^{206}Pb/^{238}U$	596.65 ± 0.87/0.95/1.6 Ma [0.01]

Note: MSWD—mean square of weighted deviates

not reported, so the date error simplifies to ±X/Z). The MSWD (York, 1966, 1967) of the $^{206}Pb/^{238}U$ weighted mean date is calculated prior to the addition of systematic uncertainties. Date errors expressed in this form for samples in this study are listed in Table A1.

APPENDIX 2. PALEOMAGNETIC SAMPLING AND LABORATORY PROCEDURES

Seven or eight cores were sampled at each site using a Pomeroy gasoline-powered, rock-coring drill. Where drilling was impossible, several hand samples were collected instead. The paleomagnetic cores were oriented with a Brunton magnetic compass on a Pomeroy orienting fixture. Sun compass measurements were made at most localities to allow correction for local magnetic variation. The geographic coordinates for each site were obtained from a handheld global positioning system (GPS) receiver and are listed in Table 2.

Specimens cut from each core were analyzed at the Byrd Polar Research Center at the Ohio State University paleomagnetism laboratory. An AGICO JR5A magnetometer was used to measure the natural remanent magnetization of one or more specimens from each core. Separate pilot samples were progressively demagnetized using stepwise alternating field and thermal techniques to determine which procedure worked best, and remaining samples were demagnetized accordingly. Only thermal methods were used for the red Squantum siltstones. During alternating field demagnetization on a Schonstedt GSD-1 instrument, steps of generally 2–3 mT were used up to ~15 mT, after which steps of 5–10 mT were used to a maximum of 95 mT (a minimum of 10 steps). During stepwise thermal demagnetization in an ASC TD48 oven, intervals of 50 °C were used up to 500 °C, followed by smaller temperature intervals of 10–20 °C (a minimum of 14 steps). Susceptibility measurements were made on a Bartington MS2 susceptibility meter after each alternating field or thermal demagnetization step to evaluate mineralogical changes associated with heating the specimens. Principal component analysis was used to define the magnetization directions as determined by collinear segments converging toward the origin (Kirschvink, 1980) and plotted on vector component diagrams. We considered the magnetization directions to be stable (whether primary or secondary) if defined by three or more collinear points on the vector component diagrams with a maximum angular deviation value of <15° (usually <10°).

ACKNOWLEDGMENTS

We thank Lisa Gahagan for creating the reconstructions in Figure 6 using the PLATES system at the Institute for Geophysics, University of Texas at Austin. Sam Bowring and Adam Maloof provided constructive comments on the manuscript, and formal reviews by Brent Miller and Phil McCausland were extremely helpful. Material in this paper is based upon work supported by the U.S. National Science Foundation under grant nos. EAR-9725828 and EAR-0125162 to Grunow, and grant nos. EAR-9725804 and EAR-0125477 to Thompson. This is Byrd Polar Research Center Contribution 1344.

REFERENCES CITED

Alkmim, F.F., Marshak, S., and Fonseca, M.A., 2001, Assembling West Gondwana in the Neoproterozoic: Clues from the São Francisco craton region, Brazil: Geology, v. 29, p. 319–322, doi: 10.1130/0091-7613(2001)029<0319:AWGITN>2.0.CO;2.

Ault, A.K., 2003, Geology of Worlds End, Hingham, Massachusetts: Sedimentation and volcanism with the Avalonian magmatic arc [honors thesis]: Wellesley, Massachusetts, Wellesley College, 100 p.

Ault, A.K., Thompson, M.D., Grunow, A.M., and Ramezani, J., 2004, Mafic Mattapan volcanism at Worlds End, Hingham, Massachusetts: New dimensions of arc activity in the Southeastern New England Avalon Zone: Geological Society of America Abstracts with Programs, v. 36, no. 2, p. 130.

Barr, S.M., and Hegner, E., 1992, Nd isotopic compositions of felsic igneous rocks in Cape Breton Island, Nova Scotia: Canadian Journal of Earth Sciences, v. 29, p. 650–657.

Barr, S.M., and White, C.E., 1996, Contrasts in late Precambrian–early Paleozoic tectonothermal history between Avalon composite terrane sensu stricto and other possible peri-Gondwanan terranes in southern New Brunswick and Cape Breton Island, Canada, *in* Nance, R.D., and Thompson, M.D., eds., Avalonian and related peri-Gondwanan terranes of the circum–North Atlantic: Geological Society of America Special Paper 304, p. 95–108.

Barr, S.M., Davis, D.W., Kamo, S., and White, C.E., 2003, Significance of U-Pb detrital zircon ages in quartzite from peri-Gondwanan terranes, New Brunswick and Nova Scotia, Canada: Precambrian Research, v. 126, p. 123–145, doi:10.1016/S0301-9268(03)00192-X.

Basei, M.A.S., Citroni, S.B., and Siga, O., Jr., 1998, Stratigraphy and age of Fini-Proterozoic basins of Paraná and Santa Cataruba States, southern Brazil: Boletim IG-USP, Sér. Cientifica, v. 29, p. 195–216.

Bevier, M.L., White, C.E., and Barr, S.M., 1990, Late Precambrian U-Pb ages for the Brookville Gneiss, southern New Brunswick: Journal of Geology, v. 98, p. 955–965.

Billings, M.P., 1976, Geology of the Boston Basin, *in* Lyons, P.C., and Brownlow, A.H., eds., Studies in New England Geology: Geological Society of America Memoir 146, p. 5–28.

Billings, M.P., Loomis, F.B., Jr., and Stewart, G.W., 1939, Carboniferous topography in the vicinity of Boston, Massachusetts: Geological Society of America Bulletin, v. 50, p. 1867–1884.

Caby, R., and Andreopoulos-Renaud, U., 1989, Âge U-Pb à 620 Ma d'un pluton synorogenique de l'Adrar des Iforas: Conséquences pour la datation de la phase majeure de l'orogénèse pan-africaine au Mali: Paris, Comptes Rendus de l'Académie des Sciences, Ser. 2, v. 308, p. 307–314.

Caby, R., Andreopoulos-Renaud, U., and Pin, C., 1989, Late Proterozoic arc-continent and continent-continent collision in the pan-African trans-Saharan belt of Mali: Canadian Journal of Earth Sciences, v. 26, p. 1136–1146.

Chapin, C.E., and Lowell, G.R., 1979, Primary and secondary flow structures in ash-flow tuffs of the Gribbles Run paleovalley, central Colorado, *in* Chapin, C.E., and Elston, W.E., eds., Ash-flow tuffs: Geological Society of America Special Paper 180, p. 137–154.

Chute, N.E.,1966, Geology of the Norwood Quadrangle, Norfolk and Suffolk Counties, Massachusetts: U.S. Geological Survey Bulletin 1163-C, 78 p.

Chute, N.E., 1969, Bedrock geologic map of the Blue Hills Quadrangle: U.S. Geological Survey, scale 1:25,000, 1 sheet.

Cordani, U.G., Basei, M.A.S., Siga, O., Jr., and Nutman, E.A., 1999, Idades U-Pb (Shrimp) de rochas vulcanicas das Bacias de Campo Alegre, Itajai e Castro (SC e PR); Resumes: Anais da Academia Brasileira de Ciencias, v. 71, p. 835.

Cordani, U.G., Brito-Neves, B.B., and d'Agrella-Filho, M.S., 2001, From Rodinia to Gondwana: A review of the available evidence from South America: Gondwana Research, v. 4, p. 600–602, doi: 10.1016/S1342-937X(05)70402-0.

D'Agrella-Filho, M.S.F., and Pacca, I.G., 1988, Paleomagnetism of the Itajai, Castro and Bon Jardim Groups from Southern Brazil: Geophysical Journal, v. 93, p. 365–376.

DePaolo, D.J., 1981, Neodymium isotopes in the Colorado Front Ranges and crust-mantle evolution in the Proterozoic: Nature, v. 291, p. 193–196, doi: 10.1038/291193a0.

Dostal, J., Caby, R., Keppie, J.D., and Maza, M., 2002, Neoproterozoic magmatism in southwestern Algeria (Sebkha el Melah inlier): A northerly extension of the Trans-Saharan orogen: Journal of African Earth Sciences, v. 35, p. 213–225, doi: 10.1016/S0899-5362(02)00104-5.

Dott, R.E., 1961, Squantum "tillite," Massachusetts—Evidence of glaciation or subaqueous mass movements?: Geological Society of America Bulletin, v. 72, p. 1289–1306.

Emerson, B.K., 1917, Geology of Massachusetts and Rhode Island: U.S. Geological Survey Bulletin 597, 289 p.

Fryer, B.J., Kerr, A., Jenner, G.A., and Longstaffe, F.J., 1992, Probing the crust with plutons: Regional isotopic geochemistry of granitoid intrusions across insular Newfoundland, *in* Current research: Newfoundland Department of Mines and Energy, Geological Survey Branch, Report 92-1, p. 119–139.

Grunow, A.M., and Encarnacion, J.P., 2000, Cambro-Ordovician palaeomagnetic and geochronologic data from southern Victoria Land, Antarctica: Revision of the Gondwana apparent polar wander path: Geophysical Journal International, v. 141, p. 392–400, doi: 10.1046/j.1365-246x.2000.00083.x.

Hamilton, M.A., and Murphy, J.B., 2003, Tectonic significance of a Llanvirn age for the Dunn Point volcanic rocks, Avalon Terrane, Nova Scotia, Canada: Implications for the evolution of the Iapetus and Rheic oceans: Tectonophysics, v. 379, p. 199–209.

Hepburn, J.C., Hon, R., Dunning, G.R., Bailey, R.H., and Galli, K., 1993, The Avalon and Nashoba terranes (eastern margin of the Appalachian orogen in southeastern New England), *in* Cheney, J.T., and Hepburn, J.C., eds., Field trip guidebook for the Northeastern United States: Boulder, Colorado, Geological Society of America, Annual Meeting, Boston, v. 2, p. X1–X31.

Hermes, O.D., and Zartman, R.E., 1992, Late Proterozoic and Silurian alkaline plutons within the Southeastern New England Avalon Zone: Journal of Geology, v. 100, p. 477–486.

Hibbard, J.P., 2004, The Appalachian Orogen—An essay by James P. Hibbard, *in* Van der Pluijm, B.A., and Marshak, S., Earth structure: An introduction to structural geology and tectonics (2nd edition): New York, W.W. Norton, p. 582–592.

Hibbard, J.P., van Staal, C.R., Rankin, D.W., and Williams, H., 2006, Lithotectonic map of the Appalachian Orogen, Canada–United States of America: Geological Survey of Canada Map 2096A, scale 1:1,500,000.

Hirdes, W., and Davis, D.W., 2002, U-Pb geochronology of Paleoproterozoic rocks in the southern part of the Kedougou-Keniéba Inlier, Senegal, West Africa: Evidence for diachronous accretionary development of the Eburnean Province: Precambrian Research, v. 118, p. 83–89, doi: 10.1016/S0301-9268(02)00080-3.

Hoffman, P.F., 1991, Did the breakout of Laurentia turn Gondwanaland inside out?: Science, v. 252, p. 1409–1412, doi: 10.1126/science.252.5011.1409.

Global Paleomagnetic Database, I.A.G.A., http://dragon.ngu.no/.

Jaffey, A.H., Flynn, K.F., Glendenin, L.E., Bentley, W.E., and Essling, A.M., 1971, Precision measurement of half-lives and specific activities of ^{235}U and ^{238}U: Physical Review, v. C4, p. 1889–1906.

Johnson, R.J.E., and Van der Voo, R., 1986, Paleomagnetism of the Late Precambrian Fourchu Group, Cape Breton Island, Nova Scotia: Canadian Journal of Earth Sciences, v. 23, p. 1673–1685.

Johnson, R.J.E., and Van der Voo, R., 1990, Pre-folding magnetization reconfirmed for the Late Ordovician–Early Silurian Dunn Point Volcanics, Nova Scotia: Tectonophysics, v. 178, p. 193–205, doi: 10.1016/0040-1951(90)90146-Y.

Karabinos, P., and Gromet, P., 1993, Applications of single-grain zircon evaporation analyses to detrital grain studies and age discrimination in igneous suites: Geochimica et Cosmochimica Acta, v. 57, p. 4257–4267, doi: 10.1016/0016-7037(93)90321-M.

Kaye, C.A., 1980, Bedrock geologic map of the Boston North, Boston South, and Newton Quadrangles: U.S. Geological Survey Map MF1241, scale 1:24,000.

Kaye, C.A., and Zartman, R.E., 1980, A late Proterozoic Z to Cambrian age for the stratified rocks of the Boston Basin, Massachusetts, *in* Wones, D.R., ed., The Caledonides in the USA: Blacksburg, Virginia Polytechnic Institute and State University Memoir 2, p. 257–261.

Keppie, J.D., and Ortega-Gutiérrez, F., 1995, Provenance of Mexican terranes: Isotopic constraints: International Geology Review, v. 37, p. 813–824.

Keppie, J.D., Davis, D.W., and Krogh, T.E., 1998, U-Pb geochronological constraints on Precambrian stratified units in the Avalon Composite Terrane of Nova Scotia, Canada: Tectonic implications: Canadian Journal of Earth Sciences, v. 35, p. 222–236, doi: 10.1139/cjes-35-3-222.

Keppie, J.D., Dostal, J., Ortega-Gutiérrez, F., and Lopez, F., 2001, A Grenvillian arc on the margin of Amazonia: Evidence from the southern Ouxacan Complex, southern Mexico: Precambrian Research, v. 112, p. 165–181, doi: 10.1016/S0301-9268(00)00150-9.

Kerr, A., Jenner, G.A., and Fryer, B.J., 1995, Sm-Nd isotopic geochemistry of Precambrian to Paleozoic granitoid suites and the deep-crustal structure of the southeast margin of the Newfoundland Appalachians: Canadian Journal of Earth Sciences, v. 32, p. 224–245.

Kirschvink, J.L., 1980, The least-squares line and plane and the analysis of palaeomagnetic data: Geophysical Journal of the Royal Astronomical Society, v. 62, p. 699–718.

Kirschvink, J.L., Ripperdan, R.L., and Evans, D.A., 1997, Evidence for large-scale reorganization of Early Cambrian continental masses by inertial interchange true polar wandering: Science, v. 277, p. 541–545, doi: 10.1126/science.277.5325.541.

Knoll, A.H., Walter, M.R., Narbonne, G.M., and Christie-Blick, N., 2004, A new period for the geologic time scale: Science, v. 305, p. 621–622, doi: 10.1126/science.1098803.

Krogh, T.E., 1973, A low-contamination method for hydrothermal decomposition of zircon and extraction of U and Pb for isotopic age determinations: Geochimica et Cosmochimica Acta, v. 37, p. 485–494, doi: 10.1016/0016-7037(73)90213-5.

Krogh, T.E., 1982, Improved accuracy of U-Pb zircon ages by the creation of more concordant systems using an air abrasion technique: Geochimica et Cosmochimica Acta, v. 46, p. 637–649, doi: 10.1016/0016-7037(82)90165-X.

Krogh, T.E., Strong, D.F., O'Brien, S.J., and Papezik, V.S., 1988, Precise U-Pb zircon dates from the Avalon terrane in Newfoundland: Canadian Journal of Earth Sciences, v. 25, p. 442–453.

LaForge, L., 1932, Geology of the Boston area, Massachusetts: U.S. Geological Survey Bulletin 839, 105 p.

Lawver, L., and Scotese, C.R., 1987, A revised reconstruction of Gondwanaland, *in* McKenzie, G.D., ed., Gondwana Six: Structure, Tectonics, and Geophysics: American Geophysical Union Monograph 40, p. 17–23.

Lenk, C., Strother, P.K., Kaye, C.A., and Barghoorn, E.S., 1982, Precambrian age of the Boston Basin: New evidence from microfossils: Science, v. 216, p. 619–620, doi: 10.1126/science.216.4546.619.

Ludwig, K.R., 1980, Calculation of uncertainties of U–Pb isotope data: Earth and Planetary Science Letters, v. 46, p. 212–220, doi: 10.1016/0012-821X(80)90007-2.

Ludwig, K.R., 1991, Isoplot—A plotting and regression program for radiogenic isotope data: U.S. Geological Survey Open-File Report 91-445.

Ludwig, K.R., 1998, On the treatment of concordant uranium-lead ages: Geochimica et Cosmochimica Acta, v. 62, p. 665–676, doi: 10.1016/S0016-7037(98)00059-3.

MacNiocaill, C., van der Pluijm, B.A., Van der Voo, R., and McNamara, A.K., 2002, Discussion and reply: West African proximity of the Avalon terrane in the latest Precambrian, Discussion: Geological Society of America Bulletin, v. 114, p. 1051–1052, doi: 10.1130/0016-7606(2002)114<1051:R>2.0.CO;2.

Magee, C.W., and Gromet, L.P., 1996, Ages of detrital zircons from the Blackstone Group, RI: Insights into the history of the Esmond-Dedham terrane prior to 620 Ma: Geological Society of America Abstracts with Programs, v. 28, no. 3, p. 77.

Mattinson, J.M., 2000, Revising the "gold standard"—The uranium decay constants of Jaffey et al., 1971: Eos (Transactions, American Geophysical Union), Spring Meeting Supplement, Abstract V61–A02.

Mattinson, J.M., 2005, Zircon U–Pb chemical-abrasion (CA-TIMS) method: Combined annealing and multi-step dissolution analysis for improved precision and accuracy of zircon ages: Chemical Geology, v. 220, p. 47–56, doi: 10.1016/j.chemgeo.2005.03.011.

McFadden, P.L., and McElhinny, M.W., 1990, Classification of the reversal test in palaeomagnetism: Geophysical Journal International, v. 103, p. 725–729.

McNamara, A.K., MacNiocaill, C., van der Pluijm, B.A., and Van der Voo, R., 2001, West African proximity of the Avalon terrane in the latest Precambrian: Geological Society of America Bulletin, v. 113, p. 1161–1170,doi: 10.1130/0016-7606(2001)113<1161:WAPOTA>2.0.CO;2.

Meert, J.G., and Van der Voo, R., 2001, Comment on 'New paleomagnetic result from Vendian red sediments in Cisbaikalia and the problem of the relationship of Siberia and Laurentia in the Vendian' by S.A. Pisarevsky, R.A. Komissarova, and Khramov, A.N.: Geophysical Journal International, v. 146, p. 867–870, doi: 10.1046/j.0956-540x.2001.01474.x.

Morell, K.D., Thompson, M.D., and Kaplin, J., 2004, Structural history of the Cambridge Argillite: Insights from tunnels near Deer Island, Boston Harbor, Massachusetts: Geological Society of America Abstracts with Programs, v. 36, no. 2, p. 138.

Murphy, J.B., Keppie, J.D., Dostal, J., and Cousens, B.L., 1996, Repeated late Neoproterozoic–Silurian lower crustal melting beneath the Antigonish Highlands, Nova Scotia: Nd isotopic evidence and tectonic interpretations, *in* Nance, R.D., and Thompson, M.D., eds., Avalonian and related peri-Gondwanan terranes of the circum–North Atlantic: Geological Society of America Special Paper 304, p. 109–120.

Murphy, J.B., Nance, R.D., and Keppie, J.D., 2002, Discussion and reply: West African proximity of the Avalon terrane in the latest Precambrian, Discussion: Geological Society of America Bulletin, v. 114, p. 1049–1050, doi: 10.1130/0016-7606(2002)114<1049:DARWAP>2.0.CO;2.

Murphy, J.B., Pisarevsky, S.A., Nance, R.D., and Keppie, J.D., 2004, Neoproterozoic–Early Paleozoic evolution of peri-Gondwanan terranes: Implications for Laurentia-Gondwana connections: International Journal of Earth Sciences, v. 93, p. 659–682, doi: 10.1007/s00531-004-0412-9.

Nance, R.D., and Murphy, J.B., 1994, Contrasting basement isotopic signatures and the palinspastic restoration of peripheral orogens: Example from the Neoproterozoic Avalonian-Cadomian belt: Geology, v. 22, p. 617–620, doi: 10.1130/0091-7613(1994)022<0617:CBISAT>2.3.CO;2.

Nance, R.D., and Murphy, J.B., 1996, Basement isotopic signatures and Neoproterozoic paleogeography of Avalonian-Cadomian and related terranes in the circum–North Atlantic, *in* Nance, R.D., and Thompson, M.D., eds., Avalonian and related peri-Gondwanan terranes of the circum–North Atlantic: Geological Society of America Special Paper 304, p. 333–346.

O'Brien, S.J., Dunning, G.R., Dubé, B., O'Driscoll, C.F., Sparkes, B., Israel, S., and Ketchum, J., 2001, New insights into the Neoproterozoic geology of the central Avalon Peninsula (Parts of NTS map area 1N/6, 1N/7 and 1N/3), eastern Newfoundland: Newfoundland Department of Mines and Energy Geological Survey Report 2001-1, p. 169–189.

Ortega-Obregón, C., Keppie, J.D., Solari, L.A., Ortega-Gutiérrez, F., Dostal, J., López, R., Ortega-Rivera, A., and Lee, J.W.K., 2004, Geochronology and geochemistry of the approximately 917 Ma, calc-alkaline Etla granitoid pluton (Ouaxaca, southern Mexico): Evidence of post-Grenvillian subduction along the northern margin of Amazonia: International Geology Review, v. 45, p. 596–610.

Pettijohn, F.J., 1957, Sedimentary rocks: New York, Harper & Row, 718 p.

Pimentel, M.M., and Fuck, R.A., 1992, Neoproterozoic crustal accretion in central Brazil: Geology, v. 20, p. 375–379, doi: 10.1130/0091-7613(1992)020<0375:NCAICB>2.3.CO;2.

Pimentel, M.M., Whitehouse, M.J., Viana, M.d.G., Fuck, R.A., and Machado, N., 1997, The Mara Rosa Arc in the Tocantins Province: Further evidence for Neoproterozoic crustal accretion in central Brazil: Precambrian Research, v. 81, p. 299–310.

Pisarevsky, S.A., Komissarova, R.A., and Khramov, A.N., 2000, New paleomagnetic results from Vendian red sediments in Cisbaikalia and the problem of the relationship of Siberia and Laurentia in the Vendian: Geophysical Journal International, v. 140, p. 598–610, doi: 10.1046/j.1365-246X.2000.t01-1-00056.x.

Rast, N., and Skehan, S.J., J.W., 1983, Evolution of the Avalonian Plate: Tectonophysics, v. 100, p. 257–286.

Ruiz, J., Tosdal, R.M., Restrepo, P.A., and Murillo-Muñetón, G., 1999, Pb isotope evidence for Colombian–southern Mexico connections in the Proterozoic, *in* Ramos, V.A., and Keppie, J.D., eds., Laurentia-Gondwana connections before Pangea: Geological Society of America Special Paper 336, p. 183–197.

Saradeth, S., Soffel, H.C., Horn, P., Mueller-Sonnius, D., and Schult, A., 1989, Upper Proterozoic and Phanerozoic pole positions and Potassium-Argon (K-Ar) ages from the East Sahara craton: Geophysical Journal of the Royal Astronomical Society, v. 97, p. 209–221.

Sayles, R.W., 1914, The Squantum Tillite: Bulletin of the Museum of Comparative Zoology at Harvard College, v. 56, p. 141–175.

Sayles, R.W., and LaForge, L., 1910, The glacial origin of the Roxbury Conglomerate: Science, v. 32, p. 723–724, doi: 10.1126/science.32.829.723.

Schmitt, R.D., Trouw, R.A.J., Van Schmus, W.R., and Pimental, M.M., 2004, Late amalgamation in the central part of west Gondwana: New geochronological data and the characterization of a Cambrian collisional orogeny in the Ribeira Belt, SE Brazil: Precambrian Research, v. 133, p. 29–61, doi: 10.1016/j.precamres.2004.03.010.

Schoene, B., Crowley, J.L., Condon, D.J., Schmitz, M.D., and Bowring, S.A., 2006, Reassessing the uranium decay constants for geochronology using ID-TIMS U-Pb data: Geochimica et Cosmochimica Acta, v. 70, p. 426–445, doi: 10.1016/j.gca.2005.09.007.

Seguin, M.K., and Giasson, M.E., 1987, Metabasalts of the Harbour Main Group, eastern Newfoundland: A paleomagnetic study: Tectonophysics, v. 138, p. 197–209, doi: 10.1016/0040-1951(87)90039-4.

Seguin, M.K., and Lortie, J., 1986, Palaeomagnetism of porphyritic stocks and rhyolite sills, Avalon Zone of eastern Newfoundland: Physics of the Earth and Planetary Interiors, v. 43, p. 148–159, doi: 10.1016/0031-9201(86)90082-8.

Seguin, M.K., Rao, K.V., and Deutsch, E.R., 1991, Paleomagnetism of Late Hadrynian Fourchu Gabbro, southern Cape Breton Island, Nova Scotia: Journal of Geomagnetism and Geoelectricity, v. 43, p. 207–228.

Smith, C., and Hon, R., 1984, Geology, petrology and origin of the Precambrian igneous rocks in the area north of Boston, *in* Hanson, L.S., ed., Geology of the Coastal Lowland, Boston, Massachusetts to Kennebunk, Maine, 76th Annual New England Intercollegiate Geological Conference: Salem, Massachusetts, Salem State College, Department of Geological Sciences, p. 292–309.

Smith, G.W., and Socci, A.D., 1990, Late Precambrian sedimentary geology of the Boston Basin, *in* Socci, A.D., et al., eds., Geology of the composite Avalon terrane of southern New England: Geological Society of America Special Paper 245, p. 75–84.

Socci, A.D., and Smith, G.W., 1990, Stratigraphic implications of facies within the Boston Basin, *in* Socci, A.D., et al., eds., Geology of the composite Avalon terrane of southern New England: Geological Society of America Special Paper 245, p. 55–74.

Steiger, R.H., and Jäger, E., 1977, Subcommission on geochronology: Convention on the use of decay constants in geo- and cosmochronology: Earth and Planetary Science Letters, v. 36, p. 359–362, doi: 10.1016/0012-821X(77)90060-7.

Teixeira, W., Tassinari, C.C.G., Cordani, U.G., and Kawashita, K., 1989, A review of the geochronology of the Amazonian craton: Tectonic implications: Precambrian Research, v. 42, p. 213–227, doi: 10.1016/0301-9268(89)90012-0.

Thomas, R.J., Chevallier, L.P., Gresse, P.G., Harmer, R.E., Eglington, B.M., Armstrong, R.A., de Beer, C.H., Martini, J.E.J., de Kock, G.S., Macey, P.H., and Ingram, B.A., 2002, Precambrian evolution of the Sirwa window, Anti-Atlas orogen, Morocco: Precambrian Research, v. 118, p. 1–57, doi: 10.1016/S0301-9268(02)00075-X.

Thompson, M.D., 1985, Evidence for a late Precambrian caldera in Boston, Massachusetts: Geology, v. 13, p. 641–643, doi: 10.1130/0091-7613(1985)13<641:EFALPC>2.0.CO;2.

Thompson, M.D., 1993, Late Proterozoic stratigraphy and structure in the Avalonian magmatic arc southwest of Boston, Massachusetts: American Journal of Science, v. 293, p. 725–743.

Thompson, M.D., and Bowring, S.A., 2000, Age of the Squantum "Tillite," Boston Basin, Massachusetts: U-Pb zircon constraints on terminal Neoproterozoic glaciation: American Journal of Science, v. 300, p. 630–655, doi: 10.2475/ajs.300.8.630.

Thompson, M.D., and Hermes, O.D., 1990, Ash-flow stratigraphy in the Mattapan Volcanic Complex, greater Boston, Massachusetts, *in* Socci, A.D., et al., eds., Geology of the composite Avalon terrane of southern New England: Geological Society of America Special Paper 245, p. 85–95.

Thompson, M.D., Grunow, A.M., and Ramezani, J., 2003, New paleomagnetic pole from the Late Cambrian Nahant Gabbro, Nahant, Massachusetts: Implications for drift history of the Southeastern New England Avalon Zone: Geological Society of America Abstracts with Programs, v. 35, no. 3, p. 18.

Thompson, M.D., Hermes, O.D., Bowring, S.A., Isachsen, C.E., Besancon, J.B., and Kelly, K.L., 1996, Tectonostratigraphic implications of Late Proterozoic U-Pb zircon ages in the Avalon Zone of southeastern New England, *in* Nance, R.D., and Thompson, M.D., eds., Avalonian and related peri-Gondwanan terranes of the circum–North Atlantic: Geological Society of America Special Paper 304, p. 179–191.

Thompson, M.D., Grunow, A.M., Ault, A.A., and Ramezani, J., 2004, Neoproterozoic magnetization and Paleozoic overprint in the Southeastern New England Avalon Zone: Geological Society of America Abstracts with Programs, v. 36, no. 7, p. 503–504.

Torsvik, T.H., and Cocks, L.R.M., 2004, Earth geography from 400 to 250 Ma: A palaeomagnetic, faunal and facies review: Geological Society [London] Journal, v. 161, p. 555–572.

Torsvik, T.H., Smethurst, M.A., Meert, J.G., Van der Voo, R., McKerrow, W.S., Brasier, M.D., Sturt, B.A., and Walderhaug, H.J., 1996, Continental break-up and collision in the Neoproterozic and Palaeozoic; a tale of Baltica and Laurentia: Earth-Science Reviews, v. 40, p. 229–258, doi: 10.1016/0012-8252(96)00008-6.

Trindade, R.I.F., D'Agrella-Filho, M.S., Epof, I., and Brito Neves, B.B., 2006, Paleomagnetism of Early Cambrian Itabaiana mafic dikes (NE Brazil) and the final assembly of Gondwana: Earth and Planetary Science Letters, v. 244, no. 1–2, p. 361–377, doi: 10.1016/j.epsl.2005.12.039.

Tucker, R.D., and Pharaoh, T.C., 1991, U-Pb zircon ages for Late Precambrian igneous rocks in southern Britain: Geological Society [London] Journal, v. 148, p. 435–443.

Van der Voo, R., 1982, Pre-Mesozoic paleomagnetism and plate tectonics: Annual Review of Earth and Planetary Sciences, v. 10, p. 191–220, doi: 10.1146/annurev.ea.10.050182.001203.

Van der Voo, R., 1993, Paleomagnetism of the Atlantic, Tethys and Iapetus Oceans: Cambridge, UK, Cambridge University Press, 411 p.

Van der Voo, R., and Johnson, R.J.E., 1985, Paleomagnetism of the Dunn Point Formation (Nova Scotia): High paleolatitudes for the Avalon terane in the Late Ordovician: Geophysical Research Letters, v. 12, p. 337–340.

van Staal, C.R., Sullivan, R.W., and Whalen, J.B., 1996, Provenance and tectonic history of the Gander Zone in the Caledonian/Appalachian orogen: Implications for the origin and assembly of Avalon, *in* Nance, R.D., and Thompson, M.D., eds., Avalonian and related peri-Gondwanan terranes of the circum–North Atlantic: Geological Society of America Special Paper 304, p. 347–367.

Vidal, G., 1976, Late Precambrian microfossils from the Visingoe beds in southern Sweden: Fossils and Strata, v. 9, 57 p.

Vizan, H., Carney, P.T., Ixer, R.A., Tomasso, M., Mullen, R.P., and Clarke, P., 2003, Late Neoproterozoic to early Paleozoic palaeogeography of Avalonia: Some paleomagnetic constraints from Nuneaton, central England: Geological Magazine, v. 140, p. 685–705, doi: 10.1017/S001675680300832X.

Watson, G.S., 1956, A test for randomness of directions: Mon. Not: Royal Astronomical Society of Geophysics, v. 7, Supplement, p. 160–161.

Watson, G.A., and Enkin, R.J., 1993, The fold test in paleomagnetism as a parameter estimation problem: Geophysical Research Letters, v. 20, p. 2135–2137.

Weber, B., and Köhler, H., 1999, Sm/Nd, Rb/Sr and U/Pb geochronology of a Grenville terrane in southern Mexico: Origin and geological history of the Guichicovi complex: Precambrian Research, v. 96, p. 245–262, doi: 10.1016/S0301-9268(99)00012-1.

Whalen, J.B., Jenne, G.B., Currie, K.L., Barr, S.M., Longstaffe, F.J., and Hegner, E., 1994, Geochemical and isotopic characteristics of granitoids of the Avalon Zone, southern New Brunswick: Possible evidence of repeated delamination events: Journal of Geology, v. 102, p. 269–282.

York, D., 1966, Least-squares fitting of a straight line: Canadian Journal of Physics, v. 44, p. 1079–1086.

York, D., 1967, The best isochron: Earth and Planetary Science Letters, v. 2, p. 479–482, doi: 10.1016/0012-821X(67)90193-8.

Zen, E-an, 1983, Bedrock geologic map of Massachusetts: U.S. Geological Survey, scale 1:250,000, 2 sheets.

Manuscript Received 5 April 2006
Revised Manuscript Received 3 October 2006
Manuscript Accepted 26 October 2006

Printed in the USA